COHERENT CONTROL WITH FEMTOSECOND LASER PULSES

T. BAUMERT, J. HELBING, and G. GERBER*

Physikalisches Institut
Universität Würzburg
Würzburg, Germany

CONTENTS

I. INTRODUCTION

Microscopic control of the outcome of a chemical reaction, the well-defined breaking (if not formation) of one or several selected bonds in a molecule, is a long-standing dream in chemistry. Many technological advances, above all the invention and development of lasers, have therefore been welcomed in the past as a possible decisive step toward its realization.

At first it was hoped, that the precise frequency of these new light sources could be employed to selectively excite individual bonds, weakening or breaking them, thus enhancing the formation of one product and discrimi-

**Report presented by G. Gerber*

Advances in Chemical Physics, Volume 101: Chemical Reactions and Their Control on the Femtosecond Time Scale, XXth Solvay Conference on Chemistry, Edited by Pierre Gaspard, Irene Burghardt, I. Prigogine, and Stuart A. Rice.
ISBN 0-471-18048-3

nating against others. However, it was soon found that the local laser excitation of a single molecular bond is not possible using continuous-wave (CW) lasers, because the deposited energy is rapidly redistributing throughout the molecule on a very short time scale.

Only much later it was realized that the excellent coherence of laser light offers another, maybe much more powerful control parameter, which allows us to make use of quantum mechanical interference. This principle forms the basis of what is today generally referred to as coherent control.

In a first example, Brumer and Shapiro proposed to simultaneously excite an exit channel via two different excitation pathways. The wave functions corresponding to the two pathways (usually one- and three-photon excitation, $\nu_1 = 3\nu_2$) may then interfere constructively or destructively depending on the phase relation between the two lasers used [1, 2].

The availability of ultrashort laser pulses has opened up further possibilities: Ultrashort, spectrally wide femtosecond lasers provide a wide range of frequencies with a fixed phase relation in a single laser pulse. Besides allowing to deposit large amounts of energy in a specific molecular bond on a time scale too short for significant energy redistribution, femtosecond laser pulses can therefore often coherently excite several rovibrational levels of a molecule simultaneously. Tannor et al. [3, 4] suggested to let the resulting wavepacket evolve until a molecular configuration is reached that is favorable to the excitation of the desired final state by a second probe pulse. These dynamical control schemes were later improved, stimulated by advances in temporal and spectral phase shaping. Shi et al. [5], Peirce et al. [6], Shi and Rabitz [7, 8], Warren et al. [9], and Amstrup et al. [10] proposed to use phase- and amplitude-modulated femtosecond pulses and trains of pulses to control not only the time of propagation but also the specific shape of molecular wavepackets (optimal control theory). In a different approach, Chelkowski et al. [11] suggested to construct laser pulses with a frequency sweep that follows the vibrational energy spacings on a molecular potential, thus making the nuclear wave function "climb up" the vibrational ladder. The latter scheme is especially applicable when intense ultrashort lasers are employed. High laser intensities may bring another important advance in controlling chemical reactions, both by increasing the total yield and by allowing the molecule to modify itself in the intense laser field [12, 13].

Despite the expectations raised with any new scheme for coherent control, their experimental realizations have so far (like the theoretical models) been widely limited to simple molecules or even atoms. Nevertheless, the feasibility of most schemes could be demonstrated in the laboratory. The picture that presents itself is therefore encouraging in principle even though for practical applications a lot of work remains to be done. It is the inten-

tion of this chapter to summarize what has been achieved experimentally by the work performed in our own group. Several parameters have been demonstrated to influence the excitation and dissociation of (small) molecules using femtosecond laser pulses and will be treated separately: pump–probe delay time, phase relation between pump and probe pulse, phase modulation, pulse length, and laser intensity.

II. EXPERIMENT

In order to achieve coherent control in a laboratory experiment, three major requirements are to be met. Well-defined final states cannot be reached without the preparation of a well-defined initial state. Ultrashort, spectrally wide and intense laser pulses at different wavelengths must be produced for excitation and a good characterization of the final product states must be achieved.

To prepare well-defined initial states the molecules studied in this contribution (Na_2 and Na_3) are prepared almost completely (>90%) in the lowest vibrational level ($v'' = 0$) of their electronic ground states in a supersonic molecular beam. The apparatus used consists of two differentially pumped high-vacuum chambers with a nominal background pressure of 2×10^{-7} torr in the interaction chamber. Vibrationally cold Na_2 is produced in an oven operated between 500 and 600°C and ejected (adiabatic expansion) through a 200-μm nozzle. The Na_3 production is enhanced at higher temperatures or by coexpanding the sodium molecular beam with argon at 4 bars (seeded beam technique) [14]. The required pulses were produced in a recently set up new laser system (Fig. 1) consisting of a Ti–sapphire oscillator, chirped pulse amplification, and an optical parametric generator [travelling-wave optical amplification of superfluorescence in combination with second-harmonic generation and sum frequency mixing (TOPAS), Light Conversion]. The home built Ar^+ ion laser pumped oscillator provides 30-fs pulses at a repetition rate of 85 MHz and 2 nJ energy that are subsequently amplified at 1 kHz in a modified commercial regenerative amplifier. This delivers 90-fs, 1.2-mJ pulses of Gaussian shape at a wavelength of 790 nm and a bandwidth of 22 nm [full width at half maximum (FWHM)]. Due to the large bandwidth of this seed pulse, TOPAS can be used to produce laser pulses over a wide range of the visible spectrum that may be compressed to their bandwidth limit of about 40 fs in a prism compressor. At 618 nm, 20-μJ pulses of 40 fs duration are generated. In a Michelson-type setup the beam can be split into equal parts and realigned with a variable time delay between the two pulses. By weakly focusing with a 300-mm achromatic lens, peak intensities of approximately 10^{11} W/cm^2 are reached.

Some of the earlier experiments were carried out using our home-built colliding pulse modelocked (CPM) ring dye laser. Equipped with two excimer

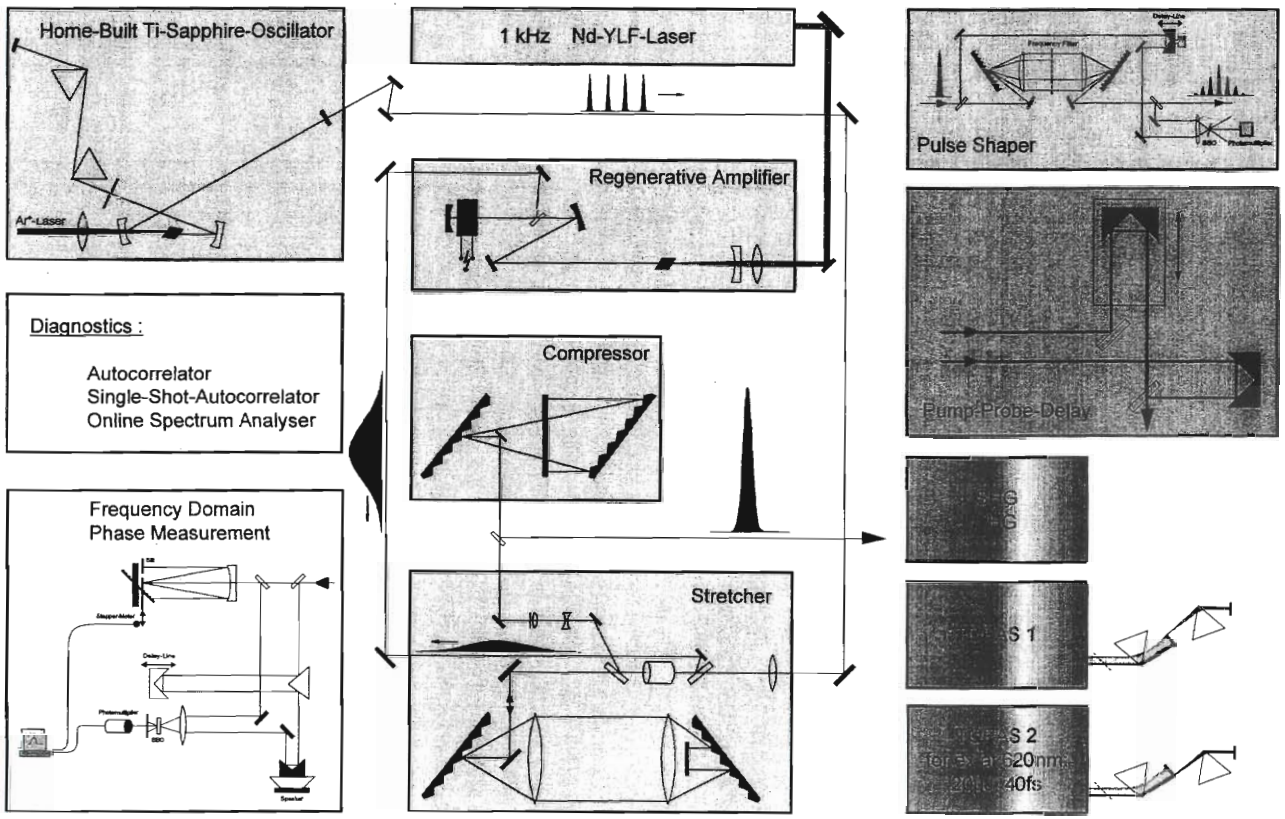

Figure 1. Overview of our new Ti--sapphire laser system, producing amplified bandwidth-limited 40-fs pulses over a wide range of the visible spectrum.

laser-pumped bow-tie amplification stages, this laser system produces 80-fs pulses of 40 μJ energy at 620 nm with a repetition rate of 100 Hz. Different wavelengths can be produced by selecting and reamplifying different frequency components from the white-light continuum generated in a cell containing methanol in a grating arrangement.

To obtain most complete information about the final states produced in our experiments, we use ion and electron time-of-flight (TOF) detection. The same linear TOF spectrometer is used for both mass- and energy-resolved measurements of ions and ionic fragments and for energy-resolved electron detection under very similar conditions. Fragment energies can be determined to an accuracy of approximately 0.1 eV. The electron spectrometer setup is calibrated by producing electrons of well-known energies via resonance-enhanced multiphoton ionization (REMPI) of atomic sodium with a nanosecond laser using several different wavelengths. Thus an energy resolution of approximately 50 meV is achieved for photoelectrons of 1 eV kinetic energy. A schematic overview of the experimental arrangement is shown in Fig. 2.

All TOF spectra are recorded with a 500-MHz digital oscilloscope (LeCroy) and averaged over several thousand laser shots. Boxcar averagers (Stanford Research) are used to integrate the signal of individual ion mass or electron energy peaks in the pump–probe experiments. The data are later corrected for laser fluctuations that are monitored by a photodiode.

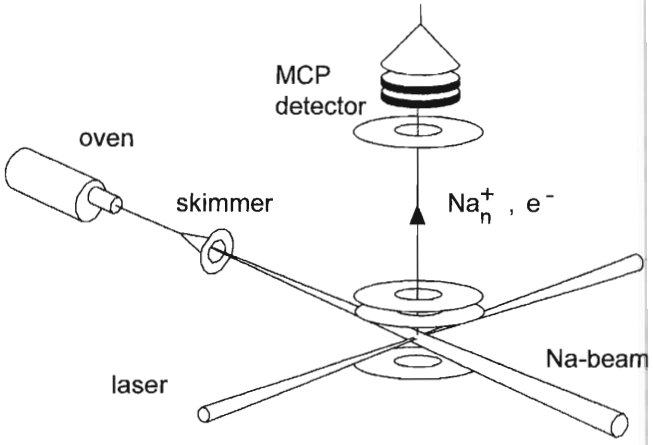

Figure 2. Schematic view of the experimental setup. The femtosecond laser beam is crossed with a cold sodium molecular beam. A linear TOF spectrometer is used for mass- and energy-resolved ion and electron detection.

III. PUMP–PROBE SCHEMES

The original idea to use lasers for the excitation of individual chemical bonds was based on the simple imagination of chemical bonds as individual springs of different strengths and characteristic frequencies. From a quantum mechanical point of view this classical picture is of course too simple; however, the path from (time-independent) quantum mechanics (energy eigenstates smeared out in space) to classical trajectory dynamics was pointed out as early as 1926 by Schrödinger [15]. When several quantum mechanical eigenstates are coherently excited with fixed phase relations, the resulting wave function resembles a wavepacket localized in space, which propagates according to the classical equations of motion. Thus in order to stretch or squeeze individual chemical bonds in the classical sense, one must coherently couple vibrational levels to form a wavepacket for which femtosecond laser pulses with their intrinsically large bandwidth are ideally suited. This was first demonstrated experimentally by Dantus et al. [16], who observed the propagation of a vibrational wavepacket on the B state of I_2.

A beautiful experiment demonstrating coherent control in the sense of the Tannor–Kosloff–Rice scheme was carried out by Baumert et al. [17] using resonant three-photon ionization and fragmentation of Na_2.

Figure 3 shows the relevant potential energy curves for excitation of Na_2 near 620 nm. Ionization is predominantly due to REMPI, whereas nonresonant multiphoton processes play only a minor role. The molecule is excited from the $v'' = 0$ vibrational level of the neutral ground state to a range of vibrational levels in the $2\ ^1\Pi_g$ state resonantly enhanced by the $A\ ^1\Sigma_u^+$ state [18]. From the $2\ ^1\Pi_g$ state different photoionization and fragmentation processes are possible. Process 1 is the direct ionization into the ionic ground state $^2\Sigma_g^+$, which yields Na_2^+. Process 2 is the excitation of a bound doubly excited neutral Na_2^{**} state at large internuclear distances followed by autoionization and autoionization-induced fragmentation yielding Na($3s$) and Na^+ fragments. When an ultrashort, spectrally broad laser pulse is used for excitation, vibrational wavepackets are formed at the inner turning points of the $A\ ^1\Sigma_u^+$ and $2\ ^1\Pi_g$ potentials, which oscillate with time constants of 320 and 380 fs, respectively. A second time-delayed probe laser may then ionize either via process 2 when the $2\ ^1\Pi_g$ state wavepacket has propagated to large internuclear distances (i.e., when the Na–Na bond has stretched) or it will transfer population into the bound ionic ground state $^2\Sigma_g^+$ (process 1). This is shown in the transient Na^+ and Na_2^+ signals in Fig. 4, which were obtained using 80-fs pulses at 618 nm from our new Ti–sapphire laser system and reproduce the data published in Ref. [17]. The Na_2^+ transient has maxima each time the probe pulse is fired when the $A\ ^1\Sigma_u^+$ state wavepacket has returned to its inner turning point but shows only a very small contri-

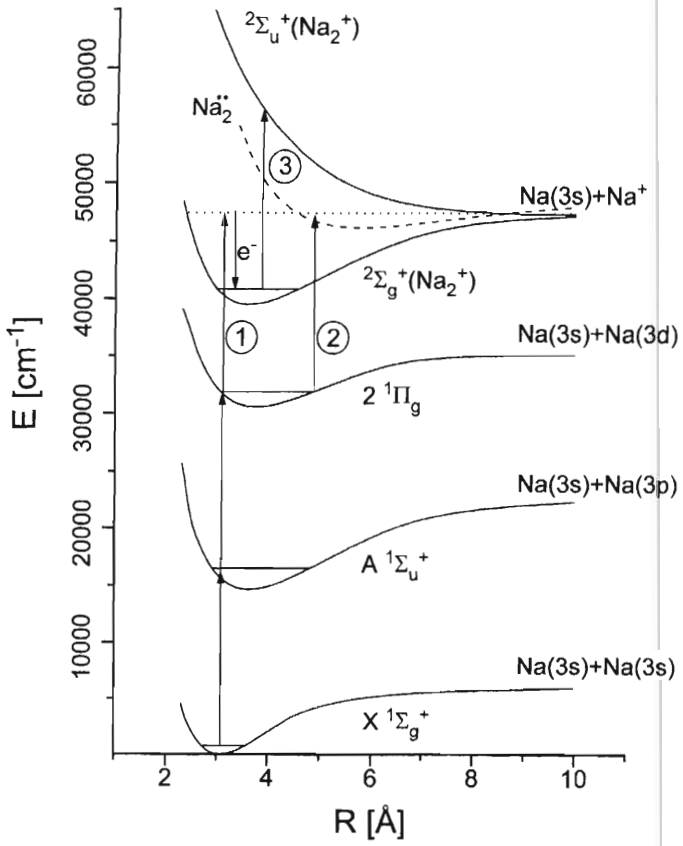

Figure 3. Potential curve diagram for the excitation, multiphoton ionization, and fragmentation of Na_2 using 620-nm photons.

bution from a wavepacket propagating on the 2 $^1\Pi_g$ state potential. This is because the Franck–Condon maximum for the 2 $^1\Pi_g$–A $^1\Sigma_u^+$ transition is found at small internuclear distances. The $^2\Sigma_g^+$–2 $^1\Pi_g$ transition on the other hand can occur over the whole range of the nuclear coordinate, thus Na_2^+ formation is insensitive to wavepacket motion on the 2 $^1\Pi_g$ potential. Since the doubly excited state Na_2^{**} can only be reached, when the 2 $^1\Pi_g$ state wavepacket is located at large internuclear distances, the Na^+ signal is modulated predominantly with the 2 $^1\Pi_g$ state frequency and is out of phase with the Na_2^+ transition. [The contribution from the A state to the Na^+ signal arises from fragmentation of Na_2^+ following direct ionization (process 3)]. The ratio Na_2^+/Na^+ can therefore be controlled by varying the time delay

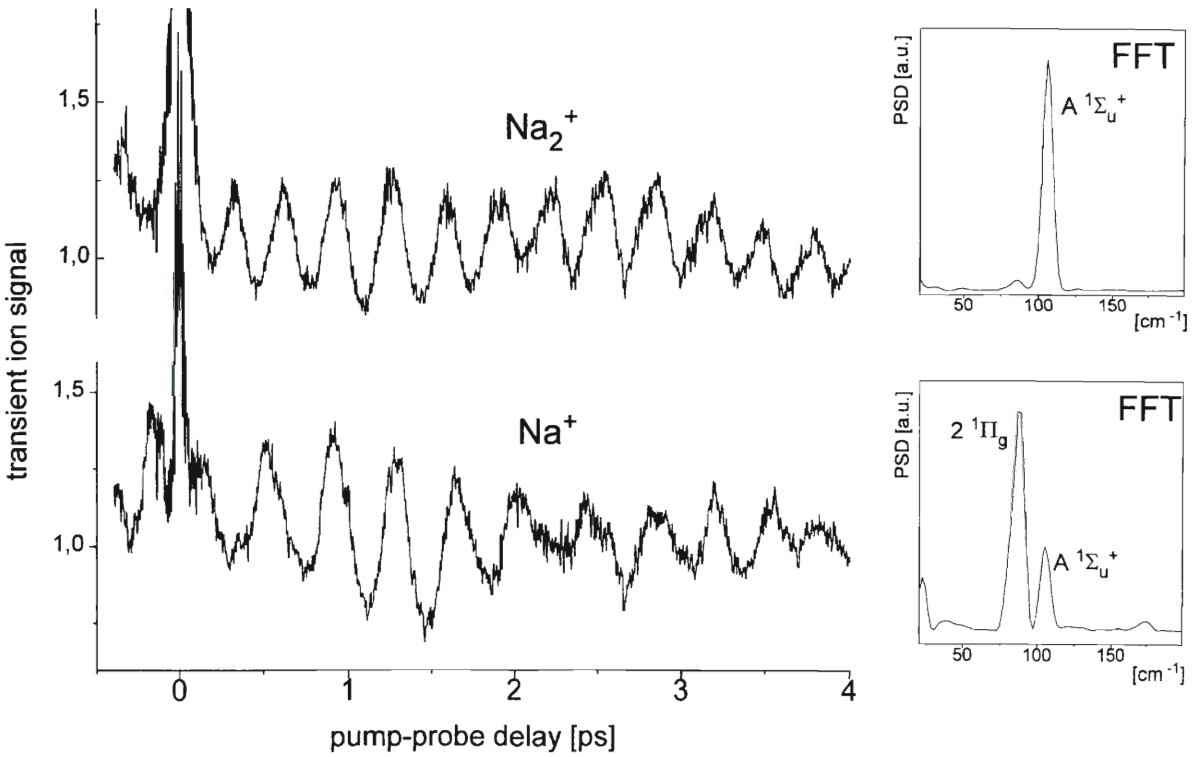

Figure 4. The Na^+ and Na_2^+ transient signals obtained from pump–probe measurements using 80-fs pulses at 618 nm. The power spectra (insets) obtained from a fast Fourier transformation (FFT) show the different frequency components of the two transients.

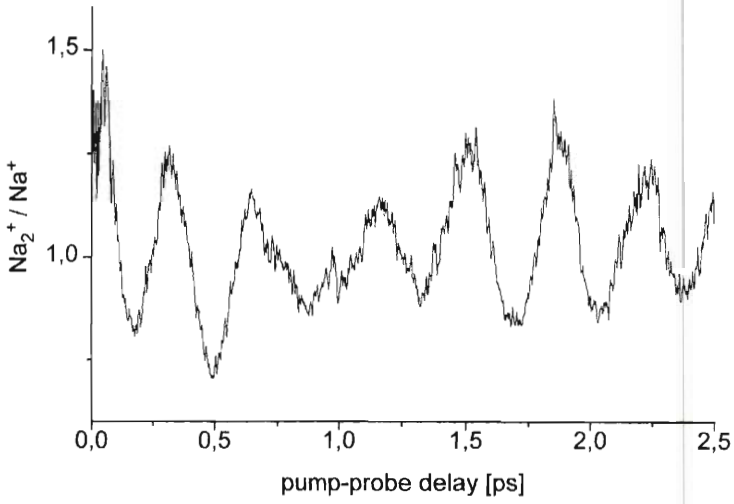

Figure 5. Ratio of Na^+ and Na_2^+ ion signals as a function of pump–probe delay using 618-nm pulses. The relative yields of fragments versus molecular ions can be controlled via the delay time.

of the ionizing pulse. Figure 5 clearly shows the oscillations of the ion to fragment signal ratio.

Coherent control by varying the time delay between a pump laser pulse that prepares an evolving wavepacket in the system and a probe laser pulse that excites the desired product state has also been demonstrated with two-photon ionization.

Figure 6 shows the relevant potential diagram of Na_2. The double-minimum state $2\ ^1\Sigma_u^+$ of the sodium dimer is used for the evolution of the molecule to the desired nuclear configuration. Due to the origin of this state from an avoided crossing between two adiabatic potential curves, a vibrational wavepacket on the $2\ ^1\Sigma_u^+$ potential created by excitation from the $v'' = 0$ level of the ground state with sufficient energy to overcome the potential barrier (340 nm) may propagate to very large internuclear distances. At large internuclear distances, the repulsive ionic state can be reached directly using 540-nm light and Na(3*s*) and Na^+ fragments are formed. Ionization at all other internuclear separations yields only Na_2^+ in its bound ground state (the additional energy is carried away by the photoelectrons). Again the ratio of Na^+/Na_2^+ shows a strong oscillatory behavior, as can be seen in Fig. 7. This time the change in ratio is even greater than observed for three-photon ionization at 620 nm [19].

Potter et al. were the first to apply this pump and control scheme to a

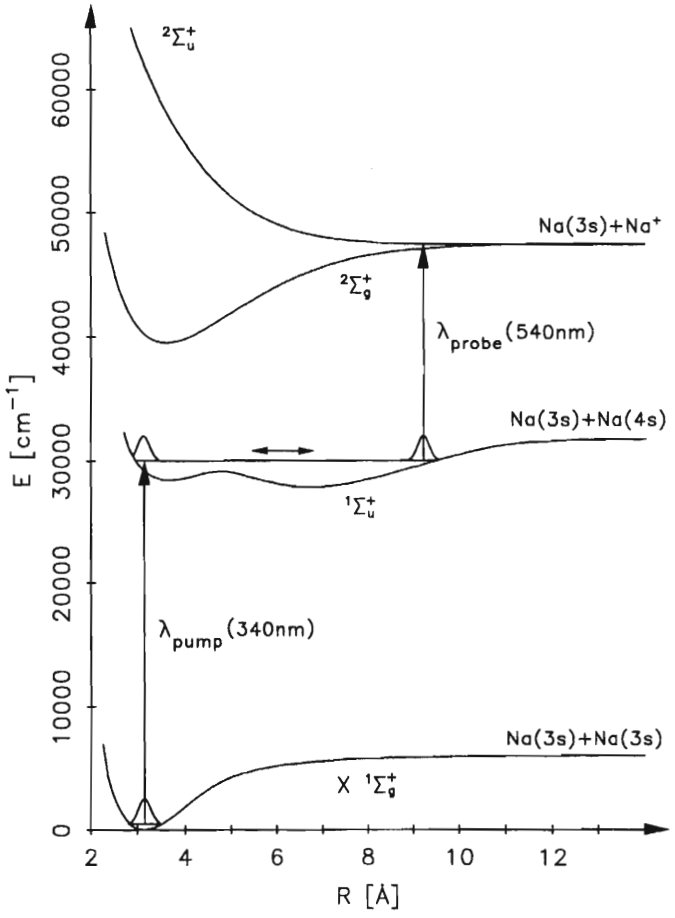

Figure 6. Potential energy curves relevant for the pump–probe experiment on the 2 $^1\Sigma_u^+$ double minimum state of Na_2. A femtosecond pump pulse forms a wavepacket at the inner turning point above the barrier. A second probe pulse (540 nm) can either only ionize (excitation of the $^2\Sigma_g^+$ ground state of Na_2^+) or ionize and fragment (excitation of the $^2\Sigma_u^+$ repulsive state) the molecule depending on the location of the wavepacket.

bimolecular (atom–molecule) reaction: Xe + I_2 → XeI + I [20]. A vibrational wavepacket was created in the *B* state of I_2 by a pump pulse. The XeI yield (detected by photoluminescence) was then observed to vary strongly as a function of time delay of a second UV-femtosecond pulse. Formation of the product XeI could therefore be switched on or off depending on the position of the wavepacket when the control pulse was applied.

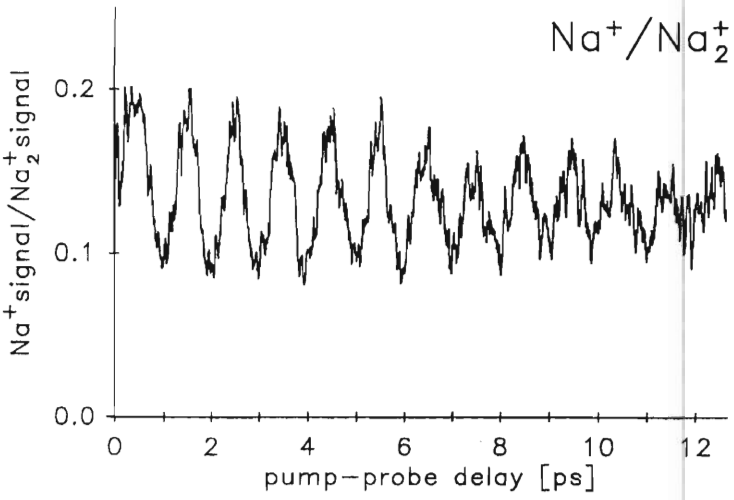

Figure 7. Ratio of Na^+ and Na_2^+ ion signals as a function of pump–probe delay for the two-photon process depicted in Fig. 6.

IV. PHASE-SENSITIVE PUMP–PROBE EXPERIMENTS

Not only the time delay between pump and probe pulses but also their phase relation was controlled in an experiment presented by Scherer et al. [21]. Using a piezocontrol, this group adjusted the time delay between two femtosecond pulses very accurately, thus keeping the relative phase constant. Both pulses excite population on the B state of I_2 in analogy to the control scheme proposed by Brumer and Shapiro [1] and beautifully demonstrated experimentally by Chen, Yin, et al. [22–24] as well as by Park, Kleinman et al. [25, 26] for CW lasers. The first wavepacket "stores" the phase information of the pump laser. Thus, each time this wavepacket returns to the Franck–Condon region at which excitation from the ground state is possible, interference is observed with the wavepacket excited by the second phase-locked laser pulse. Whether positive or negative interference occurs depends on the relative phase between the two laser pulses and the additional phase acquired by the first excited wavepacket while propagating on the molecular potential. Either relative phase angle or pump–probe delay can therefore be modified to control the final excited-state population.

When the pump–probe delay is varied slowly and continuously (i.e., both parameters are varied simultaneously), the high-frequency oscillations due to the optical phase of the wavepacket can be resolved in the transient signal, as shown by Blanchet et al. [27], who monitored the wavepacket motion and

interference on the B state of Cs_2 via two-photon ionization. The amplitude of the high-frequency oscillations is a measure of the interference between the wavepackets excited by the first and second laser pulse and is therefore large each time the first excited wavepacket has returned to its point of formation.

We have employed this phase-sensitive pump–probe technique to further investigate the multiphoton ionization of Na_2 with 618-nm femtosecond pulses as discussed in the previous paragraph and have observed the interference of the $A\ ^1\Sigma_u^+$ and $2\ ^1\Pi_g$ wavepackets created by the first pulse and those created by the second pulse in the Na_2^+ signal. The amplitude of the high-frequency oscillations in the Na_2^+ signal was obtained as a function of pump–probe delay by filtering the transient with the laser frequency. It is shown in Fig. 8 (top). Below the "averaged" Na_2^+ transient of Fig. 4 is

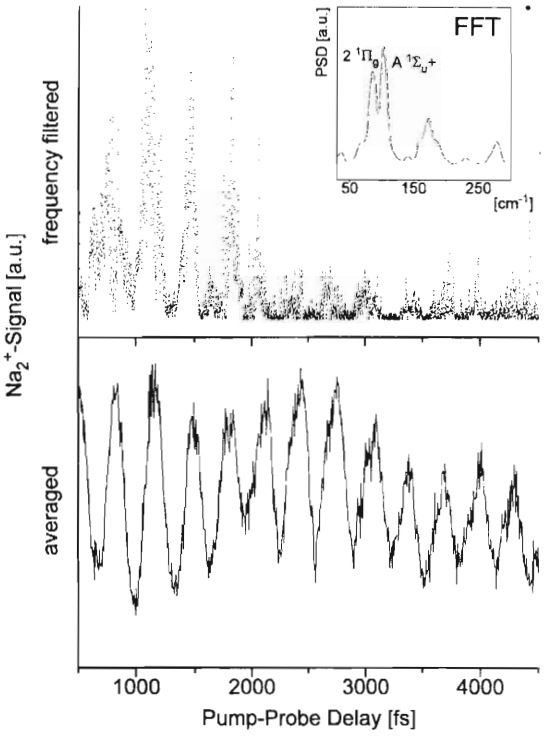

Figure 8. Frequency-filtered Na_2^+ pump–probe signal in comparison to the averaged signal of Fig. 4. The filtered signal measures by how much the Na_2^+ signal is modulated with the laser frequency. Such modulations occur when there is interference between excitation by the probe pulse and the wavepackets formed by the pump laser pulse. This interference effect causes both the $A\ ^1\Sigma_u^+$ and the $2\ ^1\Pi_g$ state wavepacket motion to be observable in the signal.

shown for comparison. As already observed in Ref. 21, information about the phase of the wavepacket (measured by the phase-sensitive or frequency-filtered transients) is lost much more quickly than information about the location of the vibrational wavepacket excited by the pump pulse (measured by the averaged transient). This may be due to the influence of rotation [21] and may limit the applicability of phase-sensitive coherent control.

On the other hand, additional spectroscopic information can be obtained by making use of this technique: The Fourier transform of the frequency-filtered transient (inset in Fig. 8) shows that the time-dependent modulations occur with the vibrational frequencies of the $A\ ^1\Sigma_u^+$ and the $2\ ^1\Pi_g$ state. In the averaged Na_2^+ transient there was only a vanishingly small contribution from the $2\ ^1\Pi_g$ state, because in the absence of interference at the inner turning point ionization out of the $2\ ^1\Pi_g$ state is independent of internuclear distance, and this wavepacket motion was more difficult to detect. In addition, by filtering the Na_2^+ signal obtained for a slowly varying pump–probe delay with different multiples of the laser frequency, excitation processes of different order may be resolved. This application is, however, outside the scope of this contribution and will be published elsewhere.

V. COHERENT CONTROL WITH PHASE-MODULATED FEMTOSECOND LASER PULSES

Shi et al. [4] showed very early theoretically that a given system may be driven very efficiently from a chosen initial state to a selected final state in a specified time interval using optimally shaped laser pulses. Kosloff et al. [28] incorporated this idea in a modified version of the Tannor–Kosloff–Rice scheme. They proposed to utilize modulation of wavepacket evolution by optimally shaped pulses on an excited-state potential energy surface to influence the selectivity of product formation in the ground state. Amstrup et al. then performed calculations involving more potential energy surfaces [10]. Only in the past few years, however, has it become possible to generate and characterize (simple) phase-modulated femtosecond laser pulses (see, e.g., Refs. 29–34) and to think about an experimental realization of the schemes proposed. Kohler et al. [35] generated vibrational wavepackets using linearly up and down chirped femtosecond laser pulses on the B state potential curve of I_2, probing by excitation of a higher lying state with a second laser at an internuclear distance slightly short of the outer turning point. The laser-induced fluorescence signal that is proportional to the population in the higher lying state was observed to exhibit a maximum after one reflection of the B state wavepacket at its outer turning point when a down chirped laser pulse was used, whereas a decrease of the signal occurred at the same pump–probe delay time for excitation with an up-chirped laser pulse. The

mechanism by which this behavior can be explained is quite general: Using chirped pulses the dispersion of a wavepacket on a potential surface can be inverted by exciting each vibrational component with the correct phase factor. While a wavepacket excited by a transform-limited pulse is spreading out in time, a wavepacket formed by a (down-) chirped laser pulse is maximally focused only after a given time delay. The application of this scheme (like all pump–probe schemes) is however limited to situations where there is no significant energy redistribution on the time scale needed for the refocusing of the wavepacket. It is therefore desirable, especially for larger molecules, to achieve the desired final configuration within the duration of a single ultrashort-phase-shaped laser pulse. Bardeen et al. managed to selectively excite vibrational wavepackets on the ground-state potential of the laser dye LD690 using strongly chirped pulses of 70 nm bandwidth (transform limit 12 fs!) [36]. The effect demonstrated in their experiment is due to the very common fact that the transition frequency between two electronic states depends on the vibrational coordinate (Franck–Condon principle). In this special case the optimal frequency for transition between the ground state of LD690 and a ring-breathing mode is decreasing with increasing vibrational coordinate. As the dye ring expands during the interaction with a laser pulse, that is, the wavepacket formed by the leading edge of the pulse on the excited-state potential propagates to larger internuclear distances, population may be transferred back down into the ground state (resonant Raman process). This is favored when the frequency within the laser pulse is decreasing in time (down chirp) and suppressed for an oppositely (up-) chirped pulse.

We can report on the observation of a strong chirp dependence of the three-photon ionization probability of Na_2 using single-phase-shaped femtosecond laser pulses [37]. Figure 9*a* shows photoelectron spectra obtained from ionizing Na_2 with up-chirped and down-chirped laser pulses at 620 nm. The chirped pulses were produced by increasing or decreasing the optical pathway in a prism sequence (SF10) that is used to compress the pulses coming out of the optical parametric generator (OPG) to their transform limit of 40 fs. The upper and lower spectra in Fig. 9*a* were obtained with linearly chirped pulses (± 3500 fs^2), which correspond to a pulse duration of approximately 240 fs. The ionization yield is seen to double when the frequency order is switched from blue first to red first in the exciting laser pulse. Note that the up- and down-chirped pulses are identical in all their pulse parameters, except for being reversed in time. This indicates that the change in the electron spectra is indeed due to the phase modulation and not to other effects such as different pulse durations or different intensity distributions.

In order to better understand the experimental results, we performed quantum mechanical calculations using the fast Fourier transform (FFT) split-operator technique, which was previously employed by Meier and Engel [38]

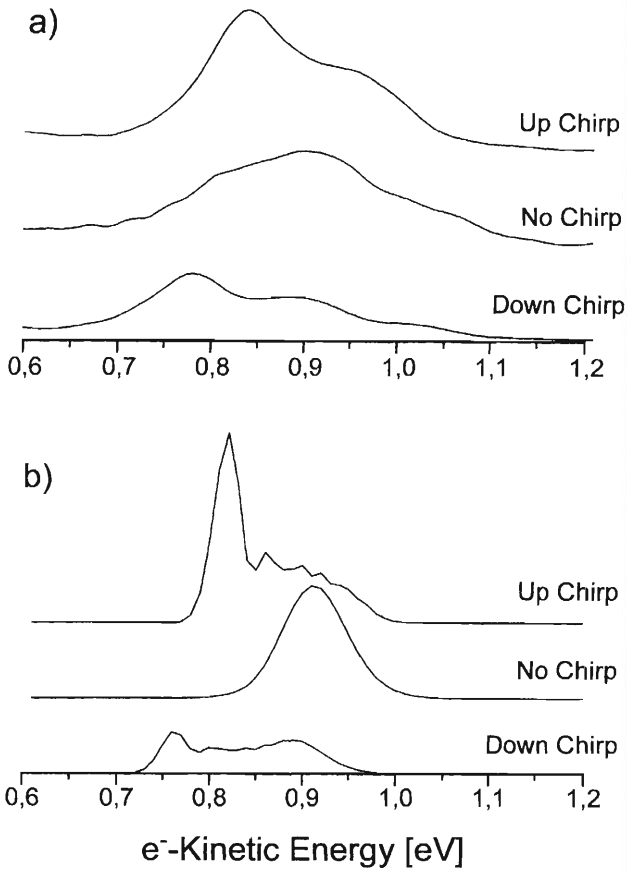

Figure 9. (*a*) Electron spectra measured with single up-chirped (+3500-fs^2) down-chirped (−3500-fs^2) and unchirped laser pulses. The transform-limited pulses of 40 fs duration are centred at a wavelength of 618 nm. The chirped pulses are of 240 fs duration. (*b*) Calculated spectra using the same parameters as (a).

to study the interaction of Na_2 with unchirped femtosecond laser pulses at 618 nm. Since the electric field of a linearly chirped Gaussian laser pulse can be written in analytical form (see, e.g., Ref. 39), the methods of Meier and Engel [38] could be easily extended to incorporate chirp effects. In accordance with the experimental conditions (the laser beam was attenuated appropriately), calculations were performed in the weak-field limit, taking into account the $X\ ^1\Sigma_g^+$, $A\ ^1\Sigma_u^+$, and $2\ ^1\Pi_g$ neutral electronic states and coupling the $2\ ^1\Pi_g$ state to the discretized continuum of the ionic ground state $^2\Sigma_g^+$ (Na_2^+). The R-independent dipole matrix elements were assumed for all

transitions. The calculated electron spectra depicted in Fig. 9*b* qualitatively reproduce the measured results. In addition, the population in the $2\ ^1\Pi_g$ state as a function of time was calculated for both chirp directions, which is shown in Fig. 10.

Since the Franck–Condon maximum for both the $A\ ^1\Sigma_u^+ \leftarrow X\ ^1\Sigma_g^+$ state transition as well as for the $2\ ^1\Pi_g \leftarrow A\ ^1\Sigma_u^+$ state transition is shifted toward the red of the central laser wavelength, the up-chirped laser pulse transfers population to the excited states earlier, whereas a down-chirped laser pulse can efficiently excite the intermediate states only with its trailing edge. For the subsequent ionization process this temporal behavior is essential. In order to achieve a high ionization yield, the population in the $2\ ^1\Pi_g$ must be high at the maximum laser intensity, which is achieved with up-chirped but not with down-chirped laser pulses.

However, Fig. 10 also yields a very surprising result. The total population transferred to the $2\ ^1\Pi_g$ state after the end of the pulse is much larger for a down-chirped laser although the ionization yield with this pulse is smaller. This is not due to population transfer to the ionic ground state since in the weak-field limit ionization does not (significantly) decrease the neutral state population. Rather a mechanism very similar to that in the experiments performed by Bardeen et al. [36] is responsible for this effect. To understand

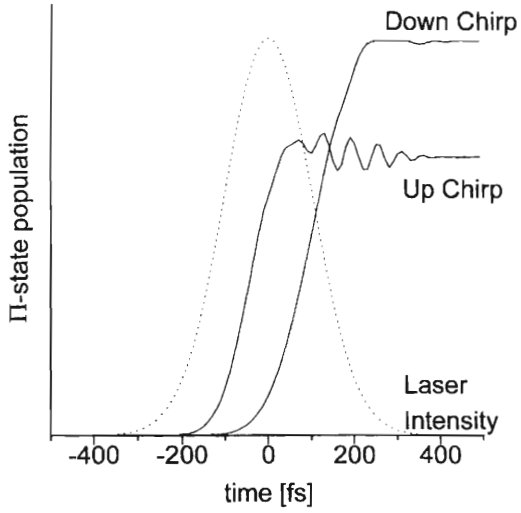

Figure 10. Temporal development of the population in the $2\ ^1\Pi_g$ state during interaction with up- and down-chirped laser pulses ($\pm 3500\ \text{fs}^2$). The chirped pulse profile is shown as a dotted line.

it, a semiclassical argument based on a difference potential analysis [40, 41] is very illuminating. By the Franck–Condon principle the nuclear kinetic energy must be conserved during an electronic transition. Thus the equation for overall energy conservation,

$$V_R(2\ ^1\Pi_g) + E_{\text{kin}}(2\ ^1\Pi_g) = V_R(A\ ^1\Sigma_u^+) + E_{\text{kin}}(A\ ^1\Sigma_u^+) + h\nu \tag{1}$$

reduces to

$$V_R(2\ ^1\Pi_g) - V_R(A\ ^1\Sigma_u^+) = h\nu \tag{2}$$

The classically allowed region for the $2\ ^1\Pi_g \leftarrow A\ ^1\Sigma_u^+$ transition is thus given by the point of intersection of the difference potential on the left-hand side of Eq. (2) with the laser energy. When a chirped laser pulse is used, the photon energy $h\nu$ is changing in time. For a down-chirped pulse the decreasing laser frequency follows the decrease in the difference potential $V_R\ (2\ ^1\Pi_g) - V_R(A\ ^1\Sigma_u^+)$, as the excited-state wavepacket propagates to larger internuclear distances. Excitation is classically allowed over a wider range of the nuclear coordinate for a down-chirped laser pulse, and the corresponding final population in the $2\ ^1\Pi_g$ state is higher. With the opposite chirp direction (up chirp) one observes a higher ionization yield while the intermediate state population is kept low. This kind of optimization is desired in coherent control schemes.

VI. INFLUENCE OF LASER PULSE DURATION

Besides the strong chirp dependence of the ionization yield observable in the electron spectra of Fig. 9, a very different electron signal is observed for unchirped 40-fs larger pulses compared to the chirped laser pulses of 240 fs duration (3500 fs^2). The short laser pulse predominantly yields electrons with kinetic energy of about 0.9 eV; the electron spectra obtained with the longer (chirped) pulses are dominated by electrons around 0.8 eV. This behavior can again be understood by a difference potential analysis, this time for the transition from the $2\ ^1\Pi_g$ state to the ionic ground state. For transitions into the ionic continuum, the emitted electron can carry away additional energy, so Eq. (2) now reads

$$V_R(^2\Sigma_g^+) - V_R(2\ ^1\Pi_g) + E_{\text{electron}} = h\nu \tag{3}$$

Since $V_R(^2\Sigma_g^+) - V_R(2\ ^1\Pi_g)$ is increasing with internuclear distance, the elec-

trons released have less kinetic energy when formed at the outer turning point of a wavepacket propagating in the 2 $^1\Pi_g$ potential than those formed at the inner turning point [42, 43]. The duration of the transform-limited 40-fs pulse is much shorter than the oscillation period (approximately 380 fs) of the excited vibrational levels of the 2 $^1\Pi_g$ state, and the wavepacket has no time to move to large internuclear distances during the laser interaction. The up- and down-chirped laser pulses, however, are of much longer duration, which allows the wavepackets to sweep the whole range of allowed internuclear distances while ionization takes place. The resulting electron spectra therefore extend to lower kinetic energies, which correspond to the outer turning point where the wavepackets spend more time. Using pulses of different duration, one can also influence the fragmentation of Na_2. As discussed in the context of the pump–probe schemes in Section III, the doubly excited state Na_2^{**}, which may subsequently yield Na(3*s*) and Na^+ ions of low kinetic energy (0.1 eV) via autoionization-induced fragmentation, is reached only at large internuclear distances (process 2 in Fig. 3). Much more energetic fragments (1.3 eV) are formed when an additional photon is absorbed by the Na_2^+ ion in its ground state, which can be reached independent of internuclear distance (process 3). Figure 11 shows the ion TOF spectra obtained with 240-fs (chirped) pulses as well as an unchirped 40-fs pulse. The broad peak at 4.5 μs is due to the low-energy fragments coming from process 2, whereas the peaks at 4.1 and 5 μs arise from fragmentation of Na_2^+ via process 3. The earlier peak is due to fragments with kinetic energy emitted in the direction of the detector; the fragments emitted in opposite direction, which are forced to turn around

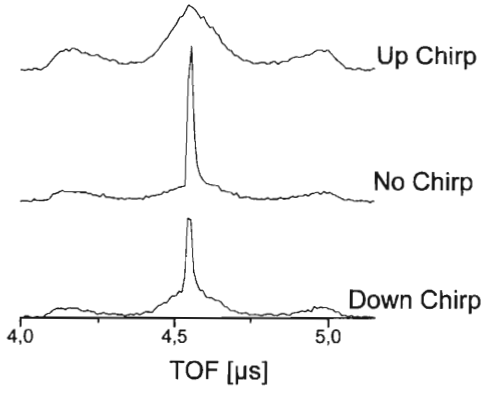

Figure 11. The Na^+ fragment TOF spectra obtained with single long (chirped) pulses of 240 fs duration and 40-fs transform-limited laser pulses at 618 nm. The ratio of low energetic versus high energetic fragments is seen to be influenced by the pulse duration.

by the extracting electric field, give rise to the later peak [18, 44]. The narrow structure on top of the low-energy fragment signal are Na^+ ions from the ionization of atomic sodium. As expected, according to the discussion of the electron signals, the Na^+ spectra show larger contributions of low-energy fragments for the longer laser pulses, since their formation involves the Na_2^{**} excitation at large internuclear distances. However, the bandwidth-limited 40-fs pulse yields almost equal amounts of fragments from processes 2 and 3.

VII. COHERENT CONTROL WITH INTENSE LASER PULSES

From a practical point of view a major disadvantage of the above control schemes is that they have been applied both theoretically and experimentally mostly in the perturbative regime, thus yielding very small amounts of the desired products. However, intense laser fields give high yields and may even be used to modify the excited molecule in such a way as to drive it to the desired final state.

Melinger et al. [45, 46] have demonstrated control of the population in $3\ ^2P_{3/2}$ and $3\ ^2P_{1/2}$ states of atomic sodium and of the B state of I_2 with intense linearly chirped laser pulses by making use of adiabatic rapid passage (ARP). They also pointed out the difficulty of achieving selectivity when many (rotational or vibrational) levels lie within the bandwidth of the laser pulses used. Chelkowski et al. [11] proposed to employ intense laser pulses with a chirp tailored in accordance with the vibrational energy spacings of a molecular potential to achieve high dissociation yields. Boers, Balling, et al. [47, 48] have demonstrated the feasibility of such an excitation on the three-level model system provided by atomic rubidium.

For a demonstration of a control scheme based on Rabi-type cycles, we look again at the Na_2 system at 620 nm as a first example. Using 80-fs laser pulses (CPM laser) of three different intensities (I_0, $0.5I_0$, and $0.1I_0$) above the perturbative regime, the Na_2^+ transients of Fig. 12 are obtained [49]. The modulation frequency of the transient signal is changing as a function of laser intensity, which can best be seen from the corresponding Fourier transforms. While at more moderate intensities mainly the A state frequency (110 cm^{-1}) contributes to the transient signal [remember that in the perturbative regime (Fig. 4), there can be no $2\ ^1\Pi_g$ state contribution to the Na_2^+ transient], the $2\ ^1\Pi_g$ state frequency (90 cm^{-1}) is beginning to dominate at higher intensities. For the highest intensity shown wavepacket motion is detected even on the electronic ground state $X\ ^1\Sigma_g^+$ (157 cm^{-1}). It is created through stimulated emission during the time the ultrashort pump pulse interacts with the molecule and is detected via direct three-photon ionization by the time-delayed probe pulse.

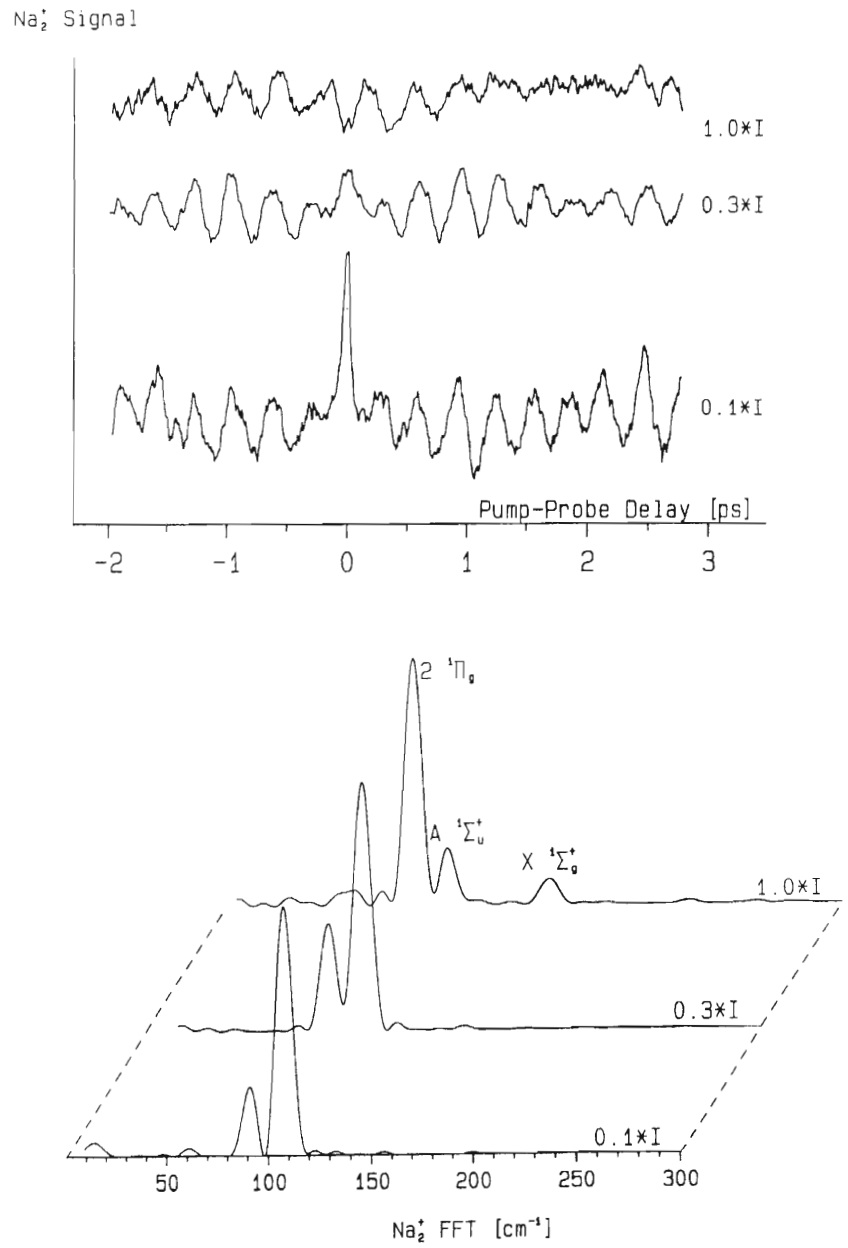

Figure 12. Transient Na_2^+ spectra as a function of delay between identical 80-fs, 620-nm pump–probe pulses for three different laser intensities (top) and corresponding Fourier transforms (bottom).

Similar transient signals were obtained from time-dependent quantum mechanical calculations performed by Meier and Engel, which well reproduce the observed behavior [49]. They show that for different laser field strengths the electronic states involved in the multiphoton ionization (MPI) are differently populated in Rabi-type processes. In Fig. 13 the population in the neutral electronic states is calculated during interaction of the molecule with 60-fs pulses at 618 nm. For lower intensities the $A\ ^1\Sigma_u^+$ state is preferentially populated by the pump pulse, and the $A\ ^1\Sigma_u^+$ state wavepacket dominates the transient Na_2^+ signal. However, for the higher intensities used in the

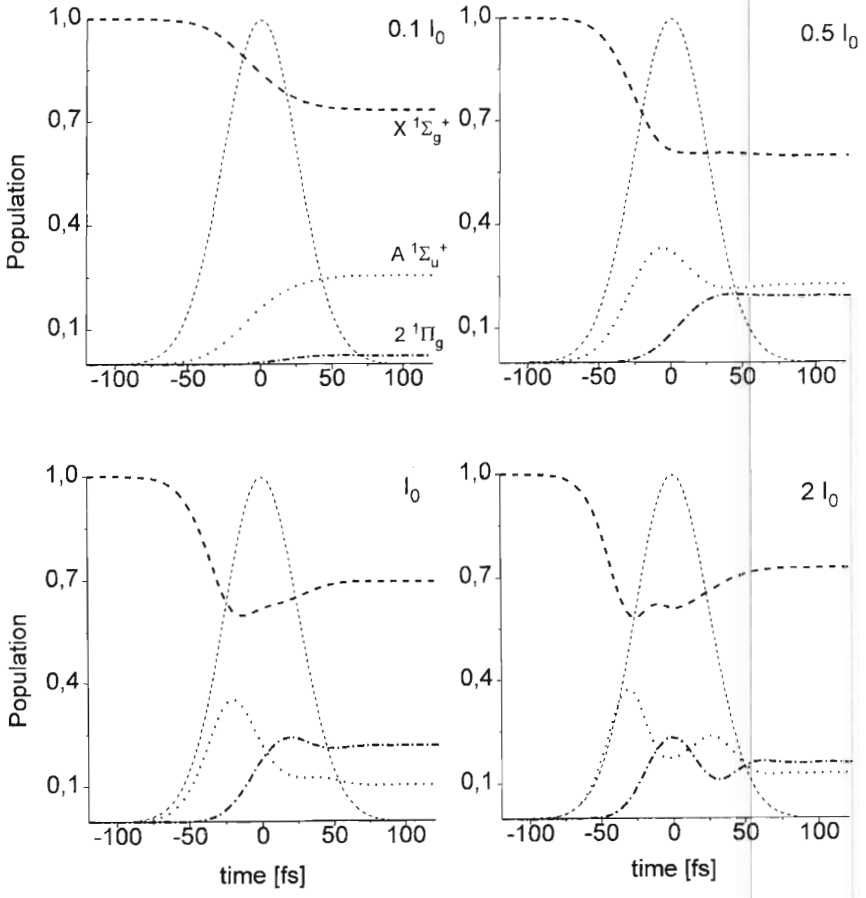

Figure 13. Population in the electronic states involved in the multiphoton ionization of Na_2 during the interaction with ultrashort laser pulses of different intensities. The calculations were performed for 60-fs pulses at 618 nm, $I_0 = 3 \times 10^{10}$ W/cm^2.

experiment the calculations indicate that the situation may well be reversed and consequently the contribution from the 2 $^1\Pi_g$ state is dominant in the measured transient signal of Fig. 12.

This shows that by varying the intensity of an ultrashort laser pulse, the population transferred to the various neutral electronic states of Na_2 can be modified. Recording the transient ion signal in a pump–probe setup can serve to monitor and control the achieved result.

The drop in Na_2^+ signal for zero pump–probe delay at the highest intensity of Fig. 12 is due to fragmentation of Na_2^+ by absorption of another photon after ionization. At higher intensities it is therefore advantageous to record the transient electron spectrum rather than the Na_2^+ signal to monitor the bound-state population. Figure 14 shows the transients of electrons formed upon direct ionization of Na_2 (process 1 in Fig. 3) recorded for three different intensities using intense 40-fs transform-limited pulses. This time the contribution of a 2 $^1\Pi_g$ state wavepacket is disappearing at the highest intensities and the ground state is eventually dominating the transient signal. Again the result can be explained by calculations of the population in the bound electronic states after the pump pulse excitation for different laser intensities (Fig. 15). They show that despite the high laser intensities the 2 $^1\Pi_g$ state population may have dropped again to zero after interaction with the pump pulse. From the calculations it can also be seen that for extremely short pulses (Fig. 15) Rabi oscillations take place predominantly between the $X\ ^1\Sigma_g^+$ and the $A\ ^1\Sigma_u^+$ electronic states while for longer pulses in Fig. 13 they are observed between the $A\ ^1\Sigma_u^+$ and 2 $^1\Pi_g$ states. This additional pulse length effect (see above) is due to the fact that the A–X transition is enhanced only at small internuclear distances. On the other hand, the $A\ ^1\Sigma_u^+$–$h\nu$ and 2 $^1\Pi_g$–$2h\nu$ dressed-state potentials calculated for a laser intensity of 5×10^{11} W/cm^2 in Fig. 16 are almost parallel, which indicates that 2 $^1\Pi_g$–$A\ ^1\Sigma_u^+$ transitions may become equally likely over a wide range of internuclear distances in intense laser fields. The fact that 2 $^1\Pi_g$–$A\ ^1\Sigma_u^+$ transitions can occur over a wide range of internuclear distances due to potential curve deformation may actually be an undesired side effect of intense laser fields, because it may lead to a loss of selectivity in pump–probe control schemes. The intensity control scheme described above can also be applied to triatomic molecules as we now demonstrate for the case of Na_3. This molecule is produced in our molecular beam apparatus at very high oven temperatures or by using argon at 4 bars as a seedgas. The excitation scheme for Na_3 using laser pulses near 620 nm can be seen in Fig. 17. The B state extends from 600 to 625 nm [50] and can be reached by one-photon excitation. A further photon can ionize Na_3, yielding Na_3^+ in its ground state. Three-photon absorption leads to fragmentation. In the ionic ground state Na_3^+ has an equilateral triangle configuration, whereas the neutral ground state and

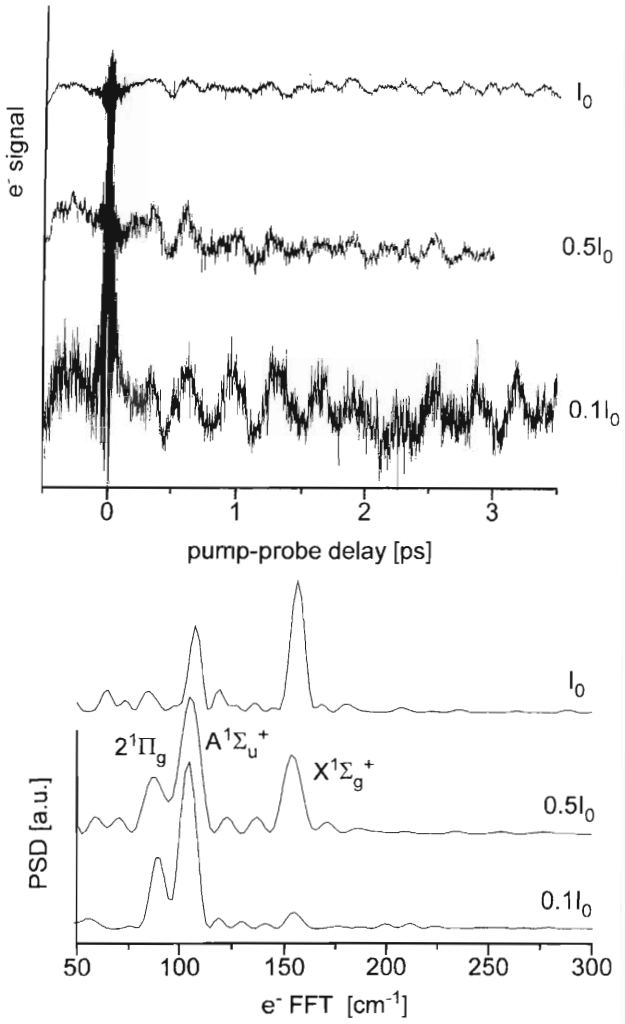

Figure 14. Transient signal of the electrons formed upon direct ionization of Na_2 (process 1 in Fig. 3) as a function of delay between identical 40-fs, 618-nm pump–probe pulses for three different laser intensities (top) and corresponding Fourier transforms (bottom).

the *B* state of Na_3 are slightly deformed due to the Jahn–Teller effect. Due to these different geometric structures, one expects configuration-dependent transition probabilities from the Franck–Condon principle. It should therefore be possible to generate and probe vibrational wavepacket motion. Figure 18 shows the Na_3^+ transient with the corresponding Fourier transform

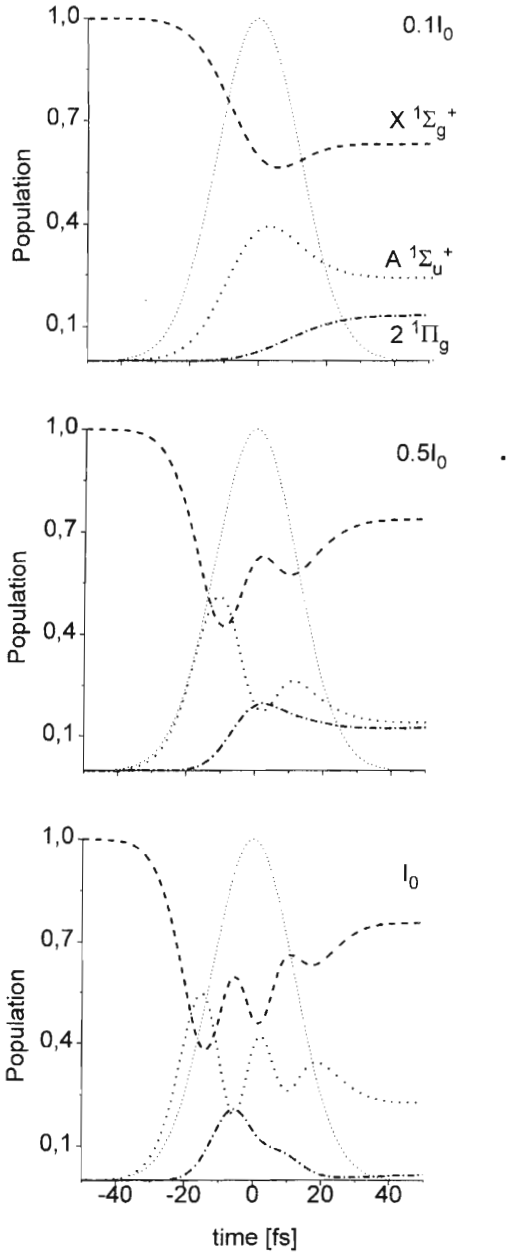

Figure 15. Like Fig. 13 but calculated for shorter (30-fs), 618-nm laser pulses, $I_0 = 2 \times 10^{11}$ W/cm^2.

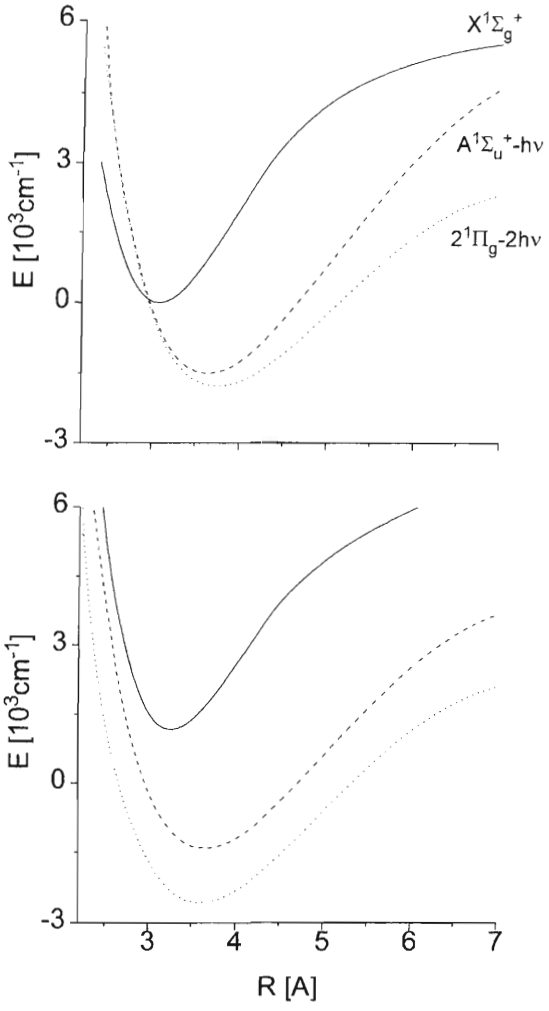

Figure 16. Diabatic (top) and adiabatic (bottom) dressed states relevant for the multiphoton ionization of Na_2 with 618-nm photons. The adiabatic dressed states were calculated for a laser intensity of 5×10^{11} W/cm^2.

obtained with strongly attenuated 80-fs pulses at 618 nm. The dominant-frequency component around 105 cm^{-1} maps the symmetric stretch oscillation (B_{ss}) of the molecule excited by the pump pulse in the B state. A smaller contribution near 72 cm^{-1} can be tentatively assigned to the asymmetric stretch (B_a) and bending (B_{as}) normal modes in the same electronic state. The fre-

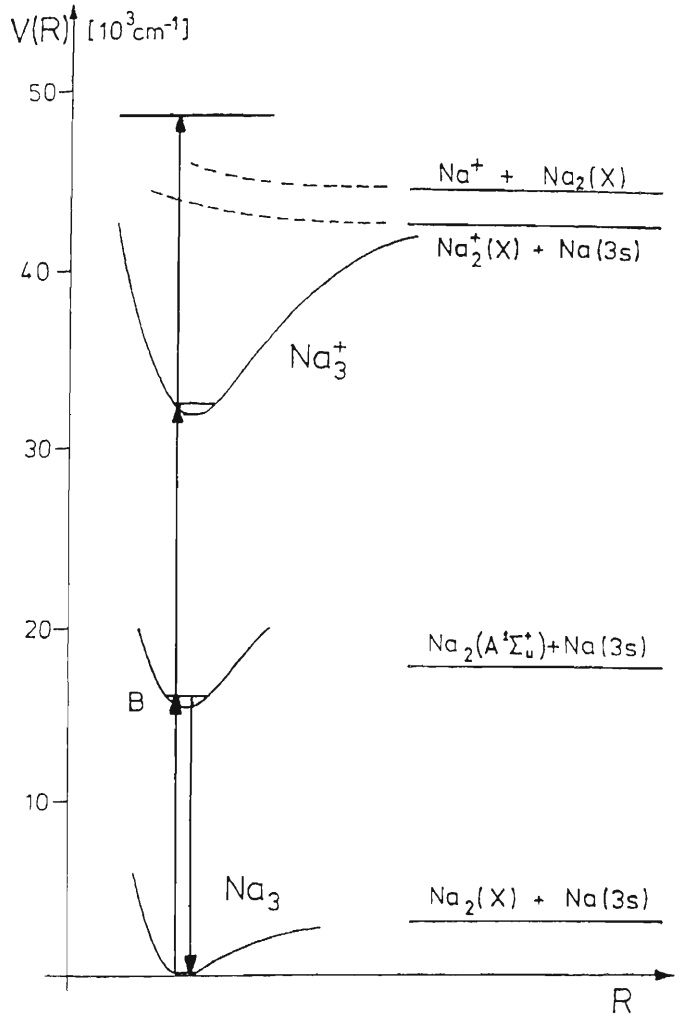

Figure 17. Schematic view of the relevant electronic states for the interaction of Na_3 with 620-nm laser pulses.

quencies observed below 40 cm^{-1} agree well with those obtained by Broyer, Delacrétaz, Rakowsky, et al. [50–53] from nanosecond laser experiments and an analysis of pseudorotation on the *B* state. Using high laser intensities the transient shown in Fig. 19 is obtained [54]. The higher intensity is immediately apparent from the drop in the Na_3^+ signal for zero pump–probe delay, which is due to three-photon fragmentation. Many more frequencies con-

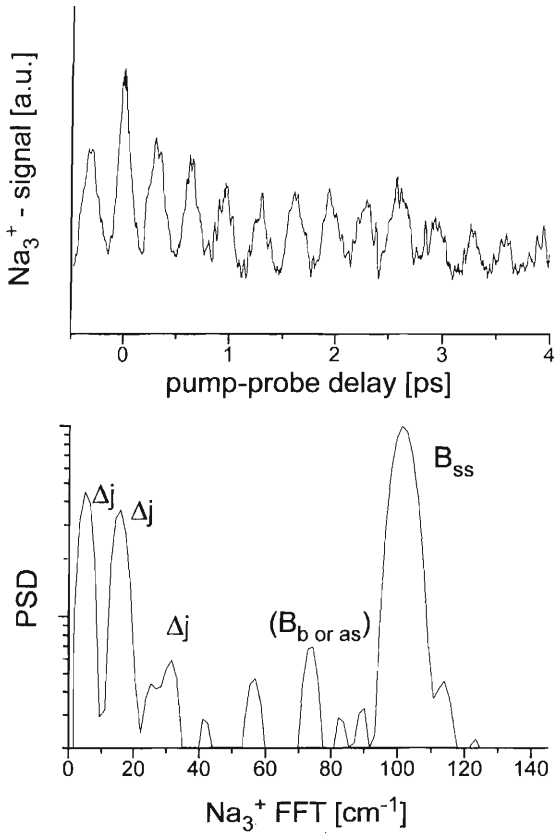

Figure 18. Transient Na_3^+ signal for strongly attenuated 80-fs pump–probe laser pulses of 620 nm. The frequencies observed in the Fourier transform are due to vibrational wavepacket motion on the *B* state potential.

tribute to the signal in this case: Besides the wavepacket propagation on the *B* state already observed at low intensities, there are now also contributions at 50, 90, and 140 cm^{-1}. These can be assigned (see again the work performed by Broyer et al. [53]) to the bending mode X_b, the asymmetric stretch mode X_{as}, and the symmetric stretch mode X_{ss} in the ground state of Na_3. This shows that the intense pump laser pulse has coherently transferred population back into the neutral ground state, thus creating wavepacket motion on this potential surface, which is subsequently probed by two-photon ionization. As in the case of Na_2, population transfer between electronic states in Rabi-type processes can therefore be controlled by varying the laser intensity and can be monitored in a pump–probe experiment.

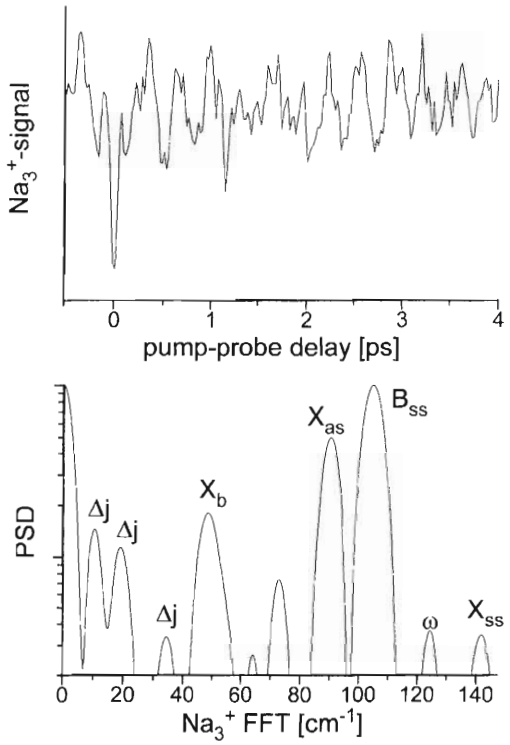

Figure 19. Transient Na_3^+ signal for intense 80-fs pump–probe laser pulses of 620 nm. In addition to the *B* state frequencies observed for low intensities, the Fourier transform now also shows contributions attributable to wavepacket motion on the ground-state potential.

VIII. CONCLUSION

In summary, we have chosen Na_2 and Na_3 to demonstrate coherent control of excited-state population, ionization yield, fragmentation, and ionic product formation using a variety of control parameters.

For a three-photon and a two-photon process we have shown that vibrational wavepacket propagation excited by an ultrashort laser pulse can be used to drive a molecule to a nuclear configuration where the desired product formation by a second probe pulse is favored (Tannor–Kosloff–Rice scheme). In both cases the relative fragmentation and ionization yield of Na_2 was controlled as a function of pump–probe delay. By varying the delay between pump and probe pulses very slowly and therefore controlling the phase relation between the two pulses, additional interference effects could be detected.

Using linearly chirped pulses, we demonstrated in a single-pulse experiment that the ionization yield of Na_2^+ can be maximized while the intermediate-state population is significantly reduced. With the help of quantum mechanical calculations and a semiclassical difference potential analysis, we elaborated that this effect is partly due to a very common variation of the transition frequency between two electronic states with internuclear distance. Making the frequency ordering of a chirped laser pulse follow this change in transition energy as a wavepacket moves along the nuclear coordinate should be very widely applicable as a technique for coherent control.

By varying the duration of a laser pulse (40 and 240 fs), the range of the nuclear coordinate swept during the interaction was varied, which is reflected by a drastic change in the electron energy distribution for the three-photon ionization of Na_2. It was shown that the pulse length can be used to influence the relative yield of high versus low energetic fragments formed via two different fragmentation processes.

Finally, coherent transfer of population between electronic states was demonstrated using intense ultrashort laser pulses of different durations. Aided by calculations, it was shown that the population in various neutral electronic states of both Na_2 and Na_3 at the end of the interaction with a laser pulse can be controlled by varying the laser intensity. A second (intense) probe laser was used to ionize the molecules. The Fourier transform obtained from the transient ion signal can be used to experimentally monitor the population distribution created by the first laser pulse.

Acknowledgments

The authors have performed the experiments presented in this contribution together with A. Assion, D. Schulz, V. Seyfried, M. Strehle, R. Thalweiser, B. Waibel, V. Weiss, and E. Wiedemann. Financial support was given by the Deutsche Forschungsgemeinschaft through SFB 276 "Korrelierte Dynamik hochangeregter atomarer und molekularer Systeme" in Freiburg.

References

1. P. Brumer and M. Shapiro, *Chem. Phys. Lett.* **126,** 541 (1986).
2. P. Brumer and M. Shapiro, *Sci. Am.* (March 1995).
3. D. J. Tannor, R. Kosloff, and S. A. Rice, *J. Chem. Phys.* **85** (10), 5805 (1986).
4. D. J. Tannor and S. A. Rice, *J. Chem. Phys.* **83,** 5013 (1985).
5. S. Shi, A. Woody, and H. J. Rabitz, *J. Chem. Phys.* **88,** 6870 (1988).
6. A. Peirce, M. Dahleh, and H. Rabitz, *Phys. Rev. A* **37,** 4950 (1988).
7. S. Shi and H. J. Rabitz, *Chem. Phys.* **139,** 185 (1989).
8. S. Shi and H. J. Rabitz, *J. Chem. Phys.* **92,** 2927 (1990).
9. W. S. Warren, H. Rabitz, and M. Dahleh, *Science* **259,** 1581 (1993).
10. B. Amstrup, R. J. Carlson, A. Matro, and S. Rice, *J. Phys. Chem.* **95,** 8019 (1991).

11. S. Chelkowski, A. D. Bandrauk, and P. B. Corkum, *Phys. Rev. Lett.* **65,** 2355 (1990).
12. A. Giusti-Suzor, X. He, O. Atabek, and F. H. Mies, *Phys. Rev. Lett.* **64,** 515 (1990).
13. X. He, O. Atabak, and A. Giusti-Suzor, *Phys. Rev. A* **38,** 5586 (1988).
14. T. Baumert and G. Gerber, *Adv. At. Molec. Opt. Phys.* **35,** 163 (1995).
15. E. Schrödinger, *Ann. Phys.* **79,** 489 (1926).
16. M. Dantus, M. H. M. Janssen, and A. H. Zewail, *Chem. Phys. Lett.* **181,** 281 (1991).
17. T. Baumert, M. Grosser, R. Thalweiser, and G. Gerber, *Phys. Rev. Lett.* **67,** 3753 (1991).
18. T. Baumert, B. Bühler, R. Thalweiser, and G. Gerber, *Phys. Rev. Lett.* **64,** 733 (1990).
19. A. Assion, T. Baumert, V. Seyfried, V. Weiss, E. Wiedenmann, and G. Gerber, *Z. Phys. D* **36,** 265 (1966).
20. E. D. Potter, J. L. Herek, S. Pedersen, Q. Liu, and A. H. Zewail, *Nature* **355,** 66 (1992).
21. N. F. Scherer, R. J. Carlson, A. Matro, M. Du, A. J. Ruggiero, V. Romero-Rochin, J. A. Cina, G. R. Fleming, and S. Rice, *J. Chem. Phys.* **95,** 1487 (1991).
22. C. Chen, Y.-Y. Yin, and D. S. Elliott, *Phys. Rev. Lett.* **64,** 507 (1990).
23. C. Chen and D. S. Elliott, *Phys. Rev. Lett.* **65,** 1737 (1990).
24. Y.-Y. Yin, C. Chen, D. S. Elliott, and A. V. Smith, *Phys. Rev. Lett.* **69,** 2353 (1992).
25. S. M. Park, S.-P. Lu, and R. J. Gordon, *J. Chem. Phys.* **94,** 8622 (1991).
26. V. D. Kleinman, L. Zhu, X. Li, and R. J. Gordon, *J. Chem. Phys.* **102,** 5863 (1995).
27. V. Blanchet, M. A. Bouchene, O. Cabrol, and B. Girard, *Chem. Phys. Lett.* **233,** 491 (1995).
28. R. Kosloff, S. A. Rice, P. Gaspard, S. Tersigni, and D. J. Tannor, *Chem. Phys.* **139,** 201 (1989).
29. A. M. Weiner, D. E. Leaird, J. S. Patel, and J. R. Wullert, *IEEE J. Quant. Electron.* **28,** 908 (1992).
30. D. H. Reitze, A. M. Weiner, and D. E. Leaird, *Appl. Phys. Lett.* **61,** 1260 (1992).
31. L. D. Noordam, W. Joosen, B. Broers, A. ten Wilde, A. Lagendijk, H. B. van Linden van den Heuvell, and H. G. Muller, *Opt. Commun.* **85,** 331 (1991).
32. M. M. Wefers and K. A. Nelson, *Opt. Lett.* **18,** 2032 (1993).
33. R. Trebino and D. Kane, *J. Opt. Soc. Am. A* **10,** 1101 (1993).
34. B. Kohler, V. V. Yakovlev, K. Wilson, J. Squier, K. W. DeLong, and R. Trebino, *Opt. Lett.* **20,** 483 (1995).
35. B. Kohler, V. V. Yakovlev, J. Che, J. L. Krause, M. Messina, K. R. Wilson, N. Schwentner, R. M. Whitnell, and Y. Yan, *Phys. Rev. Lett.* **74,** 3360 (1995).
36. C. J. Bardeen, Q. Wang, and C. V. Shank, *Phys. Rev. Lett.* **75,** 3410 (1995).
37. A. Assion, T. Baumert, J. Helbing, V. Seyfried, and G. Gerber, *Chem. Phys. Lett.* **259,** 488 (1996).
38. C. Meier and V. Engel, in *Femtosecond Chemistry*, J. Manz and L. Wöste, Eds., Verlag Chemie, Weinheim, 1995; V. Engel, *Comp. Phys. Commun.* **63,** 228 (1991).
39. S. De Silvestri, P. Laporta, and O. Svelto, *IEEE J. Quant. Electron.* **20,** 533 (1984).
40. R. S. Mulliken, *J. Chem. Phys.* **55,** 309 (1971).
41. T. Baumert, B. Buehler, M. Grosser, R. Thalweiser, E. Wiedemann, V. Weiss, and G. Gerber, *J. Phys. Chem.* **95,** 8103 (1991).
42. C. Meier and V. Engel, *Chem. Phys. Lett.* **212,** 691 (1993).
43. A. Assion, J. Helbing, V. Seyfried, and T. Baumert, *Phys. Rev. A* **54,** R4605 (1997).

44. T. Baumert, J. L. Herek, and A. H. Zewail, *J. Chem. Phys.* **99,** 4430 (1993).
45. J. S. Melinger, S. R. Gandhi, A. Hariharan, D. Goswami, and W. S. Warren, *J. Chem. Phys.* **101,** 6439 (1994).
46. J. S. Melinger, A. Hariharan, S. R. Gandhi, and W. S. Warren, *J. Chem. Phys.* **95,** 2210 (1991).
47. B. Boers, H. B. Van Linden van den Heuvell, and L. D. Noordam, *Phys. Rev. Lett.* **69,** 2062 (1992).
48. P. Balling, D. J. Maas, and L. D. Noordam, *Phys. Rev. A* **50,** 4276 (1994).
49. T. Baumert, V. Engel, C. Meier, and G. Gerber, *Chem. Phys. Lett.* **200,** 488 (1992).
50. M. Broyer, G. Delacrétaz, P. Labastie, R. L. Whetten, J. P. Wolf, and L. Wöste, *Z. Phys. D* **3,** 131 (1986).
51. G. Delacrétaz, E. R. Grant, R. L. Whetten, L. Wöste, and J. F. Zwanziger, *Phys. Rev. Lett.* **56,** 2598 (1986).
52. S. Rakowsky, F. W. Herrmann, and W. E. Ernst, *Z. Phys. D* **26** (1993).
53. M. Broyer, G. Delacrétaz, G. Q. Ni, R. L. Whetten, J. P. Wolf, and L. Wöste, *Phys. Rev. Lett.* **62,** 2100 (1989).
54. T. Baumert, R. Thalweiser, and G. Gerber, *Chem. Phys. Lett.* **209,** 29 (1993).

DISCUSSION ON THE REPORT BY G. GERBER

Chairman: S. A. Rice

L. Wöste: You showed that the above-threshold ionization process always ends at the bottom of the ionic state when exciting the system with femtosecond pulses. So, going to higher laser powers, you observe the consecutive onset of multiphotonic processes. What happens when you cross the double-ionization barrier? Is the same true for doubly charged clusters?

G. Gerber: The observed molecular ATI (above-threshold ionization) in Na_2 occurs for laser intensities above $10^{12}W/cm^2$. The observation that no additional fragmentation channels (except the $^2\Sigma_u^+$ channel) open up in Na_2^+ might explain why in femtosecond cluster experiments additional ion fragmentation channels do not show up. Within the femtosecond interaction time even under ATI conditions the lowest Franck-Condon factor (FCF-allowed) vibrational levels are the only ones observed. At even higher intensities when multiple ionization of clusters occurs, the situation can be different. This has not yet been investigated in detail.

A. H. Zewail: I have two questions for Prof. Gerber:

1. In large clusters do you observe new fragmentation pathways due to "Coulomb explosion" as observed in the nice experiments of Castleman's group?

2. What about rotationally selected wavepackets in Na_3 as reported in the new scheme shown by Leone's group for Li_2?

G. Gerber

1. For high laser intensity we observe multiply charged clusters. Even higher charged clusters undergo Coulomb explosion. As far as we have measured the initial kinetic energy release, we observe different fragment energies for different fragments.
2. At the same time a vibrational wavepacket is prepared also a rotational wavepacket is formed in our experiments. However, we have not explored that yet. It is clear what happens based upon your earlier experiments.

J. Troe: Concerning the lack of dependence of the Na_n^* lifetime on cluster size n discussed by Prof. Gerber, is it not possible that the excitation leads into repulsive excited electronic states from which the fragmentation is "direct," that is, not related to phase-space volumes and densities of states?

G. Gerber: We do observe a variation of the lifetimes τ depending on the cluster size n and also on the particular intermediate cluster resonance Na_n^* for a given size n. For these (pump-probe) decay time measurements we always selected a very specific cluster size in the detection channel! However, what is currently not understood is the irregular variation of τ for one resonance and the obviously regular behavior (independence of n) for another cluster resonance. However, what is clear is that the decay times need to be related to fragmentation processes.

J. Manz

1. Prof. Gerber has demonstrated to us three different strategies for laser control with applications to Na_2:

(i) Control of different product channels

$$\begin{aligned} Na_2 \rightarrow Na_2^* &\rightarrow Na_2^+ + e \\ &\rightarrow Na + Na^+ + e \end{aligned}$$

by choosing the selective delay time τ between the pump and control laser pulses [1], following the general strategy of Tannor et al. [2].

(ii) Control of different ionization pathways by selecting appropriate laser intensities I [3]. This strategy exploits the fact that increasing

intensities may enhance not only electronic excitation but also deexcitation (i.e., stimulated emission) processes, in particular from excited electronic states back to the ground state, thus increasing the number of photons involved in the overall photoionization process. This strategy may be supported by excitations of coherent vibrations in the electronic ground state, as predicted in Ref. 4.

(iii) Control of different ionization pathways by selective choices of the laser pulse duration t_p [5]. To the best of my knowledge, this is a new strategy, and I wish to ask Prof. Gerber for a more detailed explanation of the mechanism.

I would also like to use the opportunity and point to some of the following strategies of laser control:

(i) In Ref. 6, we combine the strategy of Tannor et al. [2] with vibrationally mediated chemistry [7], with applications to photodissociation of the model dimer $Na \cdot NH_3$.

(ii) In Ref. 8, we demonstrate the control of multiphoton ionization pathways by laser intensities I for the model system K_2. Specifically, low or moderate intensities induce three-photon ionizations via configurations with long bond lengths $r > r_e$ of K_2, whereas high intensities stimulate five-photon ionizations via excitations of a coherent wavepacket in the electronic ground state, which is then driven to a favorable new Franck–Condon window for ionization at short bond lengths $r < r_e$.

(iii) In Ref. 9, we show that different choices of laser pulse durations, specifically $t_p = 120$ fs versus 1.5 ps at low intensities, facilitate the monitoring of different vibrations of Na_3 excited to the electronic B state, specifically the symmetric stretch ν_1 versus the angular (φ) pseudorotation ν_φ. Further details of this selectivity will be explained below (see the following comment by R. de Vivie-Riedle, J. Manz, B. Reischl, and L. Wöste).

1. T. Baumert, R. Thalweiser, V. Weiss, and G. Gerber, in *Femtosecond Chemistry*, J. Manz and L. Wöste, Eds., Verlag Chemie, Weinheim, 1995, Chapter 12, p. 397.
2. D. J. Tannor and S. A. Rice, *J. Chem. Phys.* **83,** 5013 (1985); D. J. Tannor, R. Kosloff, and S. A. Rice, *J. Chem. Phys.* **85,** 5805 (1986).
3. T. Baumert and G. Gerber, *Adv. At. Molec. Opt. Phys.* **35,** 163 (1995).
4. B. Hartke, R. Kosloff, and S. Ruhman, *Chem. Phys. Lett.* **158,** 238 (1989).
5. G. Gerber, private communication. See also A. Assion, T. Baumert, J. Helbing, V. Seyfried, and G. Gerber, *Chem. Phys. Lett.*, **259,** 488 (1996).
6. C. Daniel, R. de Vivie-Riedle, M.-C. Heitz, J. Manz, and P. Saalfrank, *Int. J. Quant. Chem.* **57,** 595 (1996).
7. V. S. Letokhov, *Science* **180,** 451 (1973); F. F. Crim, *Science* **249,** 1387 (1990); J. E. Combariza, C. Daniel, B. Just, E. Kades, E. Kolba, J. Manz, W. Malisch,

G. K. Paramonov, and B. Warmuth, in *Isotope Effects in Gas-Phase Chemistry*, J. A. Kaye, Ed., *ACS Symp. Ser.* **502,** 310 (1992).

8. R. de Vivie-Riedle, J. Manz, W. Meyer, B. Reischl, S. Rutz, E. Schreiber, and L. Wöste, *J. Chem. Phys.* **100,** 7789 (1996).
9. R. de Vivie-Riedle, J. Gaus, V. Bonačić-Koutecký, J. Manz, B. Reischl, S. Rutz, E. Schreiber, and L. Wöste, in *Femtosecond Chemistry and Physics of Ultrafast Processes*, M. Chergui, Ed., World Scientific, Singapore, 1996; B. Reischl, R. de Vivie-Riedle, S. Rutz, and E. Schreiber, *J. Chem. Phys.* **104,** 8857 (1996).

2. My question to Prof. Gerber is the following: Could you please explain the different virtues of femtosecond pump-pulse experiments versus ultrashort zero electron kinetic energy (ZEKE) spectroscopy? Do they yield complementary information on the molecular dynamics or are there specific domains where one of them should be preferred with respect to the other?

G. Gerber

1. The control through variation of the femtosecond pulse duration is probably a very general scheme. In the example I discussed, using a long pulse duration (≈150 fs) we reach the outer turning point and induce the "two-electron" process. For short pulse duration (≈60 fs) we only have the channel that is open at small internuclear distances, namely the "one-electron" direct ionization. Since the (bound-free) ionization process at the inner turning point is much less probable (due to the oscillator strength) compared to the (bound–bound) process of excitation of the second electron at the outer turning point, for longer pulse durations essentially only the "two-electron" process plays a role.

2. The ZEKE detection opens up an additional and sometimes different view (compared to the ion detection channel) because of the different final states involved. This has been discussed in a recent publication [1] for the particular case of the B state dynamics of Na_3, which we had investigated.

1. A. J. Dobbyn and J. M. Hutson, *Chem. Phys. Lett.* **236,** 547 (1995).

T. Kobayashi: I have the following questions about the report by Prof. Gerber:

1. If the variation of the population as a function of delay time features damped oscillations with Rabi frequency, it is expected to see the Rabi splitting. Can this be observed?

2. Why is the two-photon ionization spectrum so broad? Is the spectrum mainly homogeneously broadened or inhomogeneously broad-

ened? If the first is the case, then why is the lifetime so long, that is, extending from a 1.1-ps component to a 215-ps component?

3. Is the intervalley scattering time on a GaAs surface faster or slower than that in bulk GaAs?

G. Gerber

1. We coherently couple different electronic states in the molecule during our intense femtosecond pulse. For higher laser intensities we induce Rabi oscillations between the different electronic states, which finally lead to a control of the population put in the different states. With an intense 50-fs pulse exhibiting an intrinsic spectral broadening of ≈30 meV we did not observe a Rabi splitting in the ion detection channel. However, in the electron detection channel (according to a theoretical paper by Engel [1]), one should observe the splitting.

2. The two-photon ionization spectrum of the Na_{20} cluster is broadened by many possible vibrational transitions. So the width is not related to the decay time of the resonance.

3. To my knowledge they are very similar, but depend on the specific surface.

1. V. Engel, *Phys. Rev. Lett.* **73,** 3207 (1994).

V. S. Letokhov: Prof. Gerber, can we exploit the analogy between the asymmetric fragmentation process ($Na_{13} \rightarrow Na_{10} + Na_3$) and the fission of nuclei?

G. Gerber: By applying two-photon ionization spectroscopy with tunable femtosecond laser pulses we recorded the absorption through intermediate resonances in cluster sizes Na_n with $n = 3, \ldots, 21$. The fragmentation channels and decay pattern vary not only for different cluster sizes but also for different resonances corresponding to a particular size n. This variation of τ and the fragmentation channels cannot be explained by collective type processes (jellium model with surface plasmon excitation) but rather require molecular structure type calculations and considerations.

U. Even: Prof. Gerber, could you follow the metal–nonmetal transition in mercury clusters?

G. Gerber: At moderate laser intensities we do see in femtosecond pump–probe experiments a very similar "slow" time and "long" time dynamics in all cluster sizes $n > 5$ up to $n \simeq 50$ (largest size investigated up to now) irrespective of the charge state of the particular Hg_n cluster. From single-pulse TOF mass spectrometry we infer that the

nonmetal–metal transition takes place for a cluster size with $n \simeq 80$ Hg atoms. Due to the transition from localized to delocalized excitations occurring in a metal, we no longer observe multiply charged Hg_n clusters at moderate laser intensities. This transition at $n \simeq 80$ is in agreement with recent calculations.

M. Chergui: My question to Prof. Gerber relates to the lifetime of the absorption resonance at 510 nm in Na_n clusters.

Since you dealt with clusters in the $n = 5, \ldots, 45$ range and, therefore, you are in the nonmetal regime (maybe even in the van der Waals regime), could one envisage that the fragmentation process occurs via a "bubble-type" mechanism whereby you are exciting a low-n Rydberg electron of a center in the cluster, which has a repulsive interaction with neighboring atoms? The impulsive blowing up of a "bubble" could give rise to a deformation that propagates to the outskirts of the cluster and leads to a boil-off of atoms. This type of mechanism has been described by Jortner and co-workers for $XeAr_n (n \leq 50)$ clusters [1, 2].

My second question is: How does the lifetime of the resonance absorption and the fragmentation process evolve if you increase the size of the cluster ($n > 45$), especially when it reaches the metal regime?

1. D. Scharf, J. Jortner, and U. Landman, *J. Chem. Phys.* **88,** 4273 (1988).
2. A. Goldberg, A. Heidenreich, and J. Jortner, *J. Phys. Chem.* **99,** 2662 (1995).

G. Gerber: I do not think this bubble picture applies to the fragmentation of particular Na_n clusters. We observed that the intermediate resonance strongly influences the time and the predominant decay channel. We did not study yet cluster sizes beyond $n = 41$. It appears that, for larger cluster sizes, no predominant picosecond decay channel exists.

D. M. Neumark: Because of the short pulses used in Prof. Gerber's experiments, the overall energy resolution is ~30 meV. What then is gained by performing ZEKE versus conventional photoelectron spectroscopy (PES) on Na_3? With PES, one could map out the Na_3 wavepacket onto the entire Na_3^+ manifold using a single ionization wavelength at each time delay.

G. Gerber: The reported experiment was done with fixed-frequency laser pulses for the pump and the probe laser. I do agree that the observation of ZEKE electrons and the dynamics of the signal using tunable femtosecond laser pulses would be of interest.

GENERAL DISCUSSION ON FEMTOCHEMISTRY: FROM ISOLATED MOLECULES TO CLUSTERS

Chairman: S. A. Rice

B. Kohler: I would like to ask two questions to Prof. Zewail. First, in your investigation of the electron transfer reaction in a benzene–I_2 complex, the sample trajectory calculations you showed appear to suggest that the charge transfer step may induce vibrationally coherent motion in I_2^-. Have you tested this possibility experimentally? My second question concerns your intriguing results on a tautomerization reaction in a model base-pair system. In many of the barrierless chemical reactions you have studied, you have been able to show that an initial coherence created in the reactant molecules is often observable in the products. In the case of the 7-azaindole dimer system your measurements indicate that reaction proceeds quite slowly on the time scale of vibrational motions (such as the N—H stretch) that are coupled to the reaction coordinate. What role do you think coherent motion might play in reactions such as this one that have a barrier?

A. H. Zewail: The observation of coherent motion in the benzene–iodine system should be related to the I_2^- motion and hopefully with better time resolution we should be able to resolve it. As for the base-pair experiment, the key motion is that of the N ·· N stretch and N—H asymmetric motions, and our time scale of observation was appropriate for the dynamics to be observed.

M. Quack: Prof. Zewail and Gerber, when you make an interpretation of your femtosecond observations (detection signal as a function of excitation), would it not be necessary to try a full quantum dynamical simulation of your experiment in order to obtain a match with your molecular, mechanistic picture of the dynamics or the detailed wavepacket evolution? Agreement between experimental observation and theoretical simulation would then support the validity of the underlying interpretation (but it would not prove it). The scheme is of the following kind:

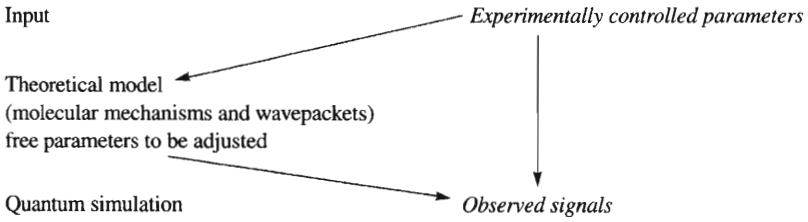

The question is then, first, how often has such a complete match between experiment and theoretical simulation been achieved? Second, are there good examples where complete simulations have been carried out but lead to two or more equally acceptable models to interpret the experimental results? I refer to this question of ambiguity also in relation to a very similar problem arising in the interpretation of non-time-resolved high-resolution spectroscopy data [1, 2], which provided in fact, the first experimental results on nontrivial three-dimensional wavepacket motion on the femtosecond time scale [3].

1. M. Quack, Chapter 27, p. 781, in *Femtosecond Chemistry*, J. Manz and L. Wöste, Eds., Verlag Chemie, Weinheim, 1995.
2. M. Quack, *Jerusalem Symp.* **24,** 47 (1991); in *Mode Selective Chemistry*, J. Jortner, R. D. Levine, and B. Pullman, Eds., Reidel, Dordrecht.
3. R. Marquardt, M. Quack, J. Stohner, and E. Sutcliff, *J. Chem. Soc. Faraday Trans. 2* **82,** 1173 (1986).

A. H. Zewail: If we solve for the molecular Hamiltonian, we will be theorists! I do, of course, understand the point by Prof. Quack and the answer comes from the nature of the system and the experimental approach. For example, in elementary systems studied by femtosecond transition-state spectroscopy one can actually clock the motion and deduce the potentials. In complex systems we utilize a variety of template-state detection to examine the dynamics, and, like every other approach, you/we use a variety of input to reach the final answer. Solving the structure of a protein by X-ray diffraction may appear impossible, but by using a number of variant diffractions, such as the heavy atom, one obtains the final answer.

B. A. Hess: In regard to the point discussed by Profs. Quack and Zewail, let me comment that, in general, inverse problems have a unique solution only under very restrictive circumstances; thus we should expect that we can find cases where the same spectroscopic data are compatible with different molecular structures.

H. Hamaguchi: I have a question directed to Prof. Zewail. You

briefly mentioned the wavepacket dynamics of the stilbene photoisomerization. What could you tell, based on this wavepacket formalism, about the stilbene photoisomerization in solution? As you know, the rate of photoisomerization increases about 100 times on going from the isolated molecule to solution. How can you account for this acceleration within the framework of the wavepacket formalism?

A. H. Zewail: There are many beautiful experiments done in the condensed phase that show such coherent nuclear wavepacket motion. For example, the work of Ruhman on I_3^- and Hochstrasser on HgI_2 and *cis*-stilbene. The latter two have shown direct analogy to the results observed in the isolated gas phase. It appears that the time scale for intermolecular couplings is somewhat longer than those of the intramolecular dynamics, even though solvent-induced dephasing and vibrational relaxation are integral parts of the dynamics. For *cis*-stilbene, the wavepacket motion indicates that the molecule is twisting, utilizing a second motion, the phenyls, in addition to the expected ethylenic torsion. As for the acceleration of the rates in solution for *trans*-stilbene this is due to the microscopic friction and the lowering of the barrier. [See A. A. Heikal, S. H. Chong, J. S. Baskin, and A. H. Zewail, *Chem. Phys. Lett.* **242,** 380 (1985).]

J.-L. Martin: Prof. Zewail, how do you expect your work on photoinduced tautomerization of base pairs to apply to the real world of DNA, where such a reaction would happen on ground-state potential surface in a water environment?

A. H. Zewail: The relationship to real-life DNA structures is certainly not known to us. However, as you can see from the paper in *Nature* [1], the transient structures have never been isolated and there is another important point. The presence of an "ionic intermediate" is possibly significant for recognition by enzymes of mutation by this mechanism, if operative.

1. M. F. Goodman, *Nature* **378,** 237 (1995); A. Donhal, S. K. Kim, and A. H. Zewail, *Nature* **378,** 260 (1995).

K. Yamanouchi: I have two comments concerning Prof. Zewail's report:

1. By using the presented second-generation gas electron diffraction apparatus, it would also be possible to probe vibrational motion in real time. Especially when a molecule is photodissociated, a series of snapshots of a diffraction pattern would facilitate understanding the photodissociation process because it describes how a molecule vibrates in the course of the separation of two frag-

ments flying apart. This vibrational motion during the dissociation process is subject to the so-called intramolecular vibrational energy redistribution (IVR), which plays a central role in a unimolecular dissociation reaction. The new gas electron diffraction experiments presented here by Prof. Zewail could have powerful potential to visualize IVR through the real-time probing.

2. In conventional gas electron diffraction experiments, an effusive beam is used in which vibrational levels of molecules are thermally populated and the width of a peak in a radial distribution curve is determined by thermally averaged mean amplitudes. When a molecular beam or a free jet is used, mean amplitudes could become small, since the contribution from the vibrationally excited levels is reduced significantly. As a consequence, sharper peaks are expected in the radial distribution curve, and the spatial resolution of the snapshot could be improved. However, it seems that the observed peaks in the radial distribution curve are considerably broad even though a molecular beam is used. There could be some reasons to have such broadened peaks in the radial distribution curve.

A. H. Zewail: Prof. Yamanouchi is correct in pointing out the relevance of ultrafast electron diffraction to the studies of vibrational (and rotational) motion. In fact, Chuck Williamson in our group [1] has considered precisely this point, and we expect to observe changes in the radial distribution functions as the vibrational amplitude changes and also for different initial temperatures. The broadening in our radial distribution function presented here is limited at the moment by the range of the diffraction sampled.

1. J. C. Williamson and A. H. Zewail, *J. Phys. Chem.* **98,** 2766 (1994).

P. Backhaus, J. Manz, and B. Schmidt:* Prof. A. H. Zewail has demonstrated to us some fascinating new pump–probe femtochemistry investigations of bimolecular reactions (e.g., Ref. 1; see also Ref. 2)

$$H + CO_2 \rightarrow HOCO^{\ddagger} \rightarrow OH + CO \qquad (1)$$

To the best of our knowledge, however, these types of "bimolecular" studies start from weakly bound precursor systems, for example,

$$IH \cdot OCO \rightarrow IH^{*} \cdot CO_2 \rightarrow I + HOCO^{\ddagger} \rightarrow I + OH + CO \qquad (2)$$

*Comment presented by J. Manz.

From the viewpoint of the van der Waals type or hydrogen-bounded reactant, these reactions may therefore be considered as "unimolecular" even though they exhibit various characteristics of bimolecular processes.

Here we wish to point to a new type of femtosecond chemistry investigations of bimolecular reactions, demonstrated first by Dantus et al. [3] for the prototype system

$$2\,Hg \rightarrow Hg_2^* \qquad (3)$$

Essentially, an ultrashort laser pulse associates two colliding reactants to a new product. In the present case, a metastable excimer Hg_2^* is formed from two mercury atoms. This photoassociation process may be considered as the reverse of photodissociation. From a theoretical point of view, the important difference between processes (2) and (3) is that the unimolecular photodissociation (2) starts from bound states, whereas the bimolecular photoassociation (3) starts from continuum states, as demonstrated by model simulations in Fig. 1 (supported by Deutsche Forschungsgemeinschaft).

1. N. F. Scherer, L. R. Khundkar, R. B. Bernstein, and A. H. Zewail, *J. Chem. Phys.* **87,** 1451 (1987); N. F. Scherer, C. Sipes, R. B. Bernstein, and A. H. Zewail, *J. Chem. Phys.* **92,** 5239 (1990); A. H. Zewail, in *Femtosecond Chemistry*, J. Manz and L. Wöste, Eds., Verlag Chemie, Weinheim, 1995, p. 15; A. H. Zewail, *J. Phys. Chem.* **100** (1996), in press.
2. S. I. Ionov, G. A. Brucker, C. Jaques, L. Valachovic, and C. Wittig, *J. Chem. Phys.* **99,** 6553 (1993); M. Alagia, N. Balucani, P. Casavecchia, D. Stranges, and G. G. Volpi, *J. Chem. Phys.* **98,** 8341 (1993); G. C. Schatz and M. S. Fitzcharles, in *Selectivity in Chemical Reactions*, J. C. Whitehead, Ed., Kluwer, Dordrecht, 1988, p. 353; E. M. Goldfield, S. K. Gray, and G. C. Schatz, *J. Chem. Phys.* **102,** 8807 (1995); D. C. Clary and G. C. Schatz, *J. Chem. Phys.* **99,** 4578 (1993), D. H. Zhang and J. Z. H. Zhang, *J. Chem. Phys.* **103,** 6512 (1995); see also L. Krim, P. Qiu, N. Halberstadt, B. Soep, and J. P. Visticot, in *Femtosecond Chemistry*, J. Manz and L. Wöste, Eds., Verlag Chemie, Weinheim, 1995, p. 433.
3. U. Marvet and M. Dantus, *Chem. Phys. Lett.* **245,** 393 (1995).
4. P. Backhaus, M. Dantus, J. Manz, and B. Schmidt, in preparation.
5. J. Koperski, J. B. Atkinson, and L. Krause, *Can. J. Phys.* **72,** 1070 (1994).
6. F. H. Mies, W. J. Stevens, and M. Krauss, *J. Molec. Spectrosc.* **72,** 303 (1978).
7. E. W. Smith, R. E. Drullinger, M. M. Hessel, and J. Cooper, *J. Chem. Phys.* **66,** 15 (1977).

J. Manz: Moreover, I have another comment on the contributions by A. H. Zewail and G. Gerber and a question to all my colleagues and, in particular, to the Chairman, Prof. S. A. Rice:

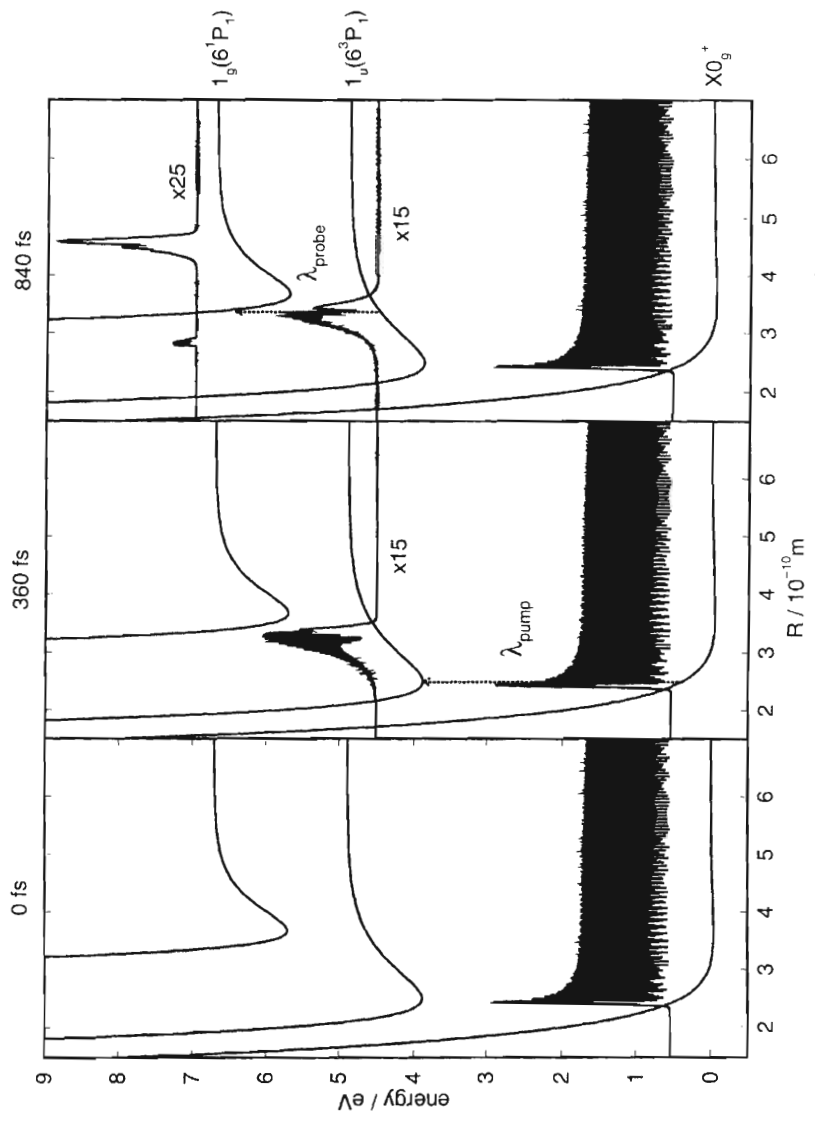
0 fs
360 fs
840 fs
energy / eV
R / 10^{-10} m
$1_g(6^1P_1)$
$1_u(6^3P_1)$
$X0_g^+$
x25
x15
x15
λ_{probe}
λ_{pump}

Figure 1. Photoassociation 2Hg → Hg_2* by ultrashort femtosecond laser pulses. The figure shows a sequence of three snapshots of the wavepacket dynamics tailored to the experiment of Marvet and Dantus [3]. At t = 0 fs, the reactants Hg(XO_g^+) are in a continuum state with energy E and rotational quantum numbers J, M. The pump laser pulse (λ_{pump} = 312 nm, $I_{max} = 2 \times 10^{11}$ W/cm^2, τ = 65 fs) creates a small fraction of dimers Hg_2* ($1_u(6^3P_1)$), and the probe pulse (λ_{pump} = 624 nm, $I_{max} = 2 \times 10^{13}$ W/cm^2, τ = 65 fs) monitors the coherent vibration of these Hg_2* (1_u) excimers by depopulation due to the $1_u \rightarrow 1_g(6^1P_1)$ transition. The remaining population of Hg_2 *(1_u) depends on the delay time of the pump and probe laser pulses (in the present case t_d = 480 fs) and is measured by fluorescence. All laser parameters are adapted to the experimental situation [3]. The present simulation is exemplary for E = 0.529 eV, J = 0, M = 0, and Boltzmann averaging over equivalent calculations for other values of E, J, M accounts for the thermal (T = 433.15 K) situation of the experiment; see Ref. 4. The potential energies and transition dipoles are adapted from Refs. 5, 6, and 7, respectively; for the $1_g \rightarrow 1_u$ transition, we assume $\mu = 1ea_0$: This does not affect the relative pump and probe signal (in arbitrary units).

Prof. G. Gerber and A. H. Zewail have presented to us three fascinating experiments on femtosecond laser control of the branching ratio of competing product channels:

$$\begin{aligned} \mathrm{Xe}\cdot\mathrm{I_2} \rightarrow [\mathrm{Xe^+}\cdots\mathrm{I^-}\cdots\mathrm{I}]^{\ddagger *} &\rightarrow \mathrm{Xe} + \mathrm{I_2} \\ &\rightarrow \mathrm{XeI}^* + \mathrm{I} \quad \text{(Ref. 1)} \qquad (1) \\ \mathrm{Na_2} \rightarrow \mathrm{Na_2}^* &\rightarrow \mathrm{Na_2}^+ + \mathrm{e} \\ &\rightarrow \mathrm{Na} + \mathrm{Na^+} + \mathrm{e} \quad \text{(Ref. 2)} \qquad (2) \\ \mathrm{NaI} \rightarrow \mathrm{NaI}^* &\rightarrow \mathrm{Na} + \mathrm{I} \\ &\rightarrow \mathrm{NaI} \quad (v \gg 0) \quad \text{(Ref. 3)} \quad (3) \end{aligned}$$

where NaI ($v \gg 0$) denotes the vibrationally excited NaI molecule in the electronic ground state. Essentially, they employ two femtosecond laser pulses with proper time delay t_d. The first pump pulse initiates ($t = 0$) a coherent nuclear motion in the electronic excited state. This is represented by a nuclear wavepacket that is driven from the molecular equilibrium configuration of the reactant at time $t = 0$ toward new configurations close to those of the products at time $t = t_d$. The second control pulse ($t = t_d$) then induces an electronic transition that serves to stabilize the desired product. Historically, it is amazing and certainly encouraging and gratifying that this type of femtosecond laser control by two femtosecond pump and control laser pulses had been predicted by Tannor et al. already in 1985 [4] (see also Ref. 5), that is, one or two years before the first femtosecond laser chemistry investigation of a chemical reaction, carried out by Zewail et al. in 1987 [6]. I should like to ask whether the experimental (see Refs. 1–3) or theoretical pioneers (see Ref. 4) or any other colleagues could point to any other experimental verifications of the Tannor–Rice–Kosloff strategy [4] beyond processes (1–3).

1. E. P. Potter, J. L. Herek, S. Pedersen, Q. Liu, and A. H. Zewail, *Nature* **355,** 66 (1992).
2. T. Baumert, R. Thalweiser, V. Weiss, and G. Gerber, in *Femtosecond Chemistry*, Vol. 2, J. Manz and L. Wöste, Eds., Verlag Chemie, Weinheim, 1995, p. 397.
3. J. L. Herek, A. Materny, and A. H. Zewail, *Chem. Phys. Lett.* **228,** 15 (1994).
4. D. J. Tannor and S. A. Rice, *J. Chem. Phys.* **83,** 5013 (1985); D. J. Tannor, R. Kosloff, and S. A. Rice, *J. Chem. Phys.* **85,** 5805 (1986).
5. S. A. Rice, *J. Chem. Phys.* **90,** 3063 (1986); S. A. Rice, Perspectives on the control of quantum many body dynamics: Application to chemical reactions, *Adv. Chem. Phys.*, **101,** (1997).
6. M. Dantus, M. J. Rosker, and A. H. Zewail, *J. Chem. Phys.* **87,** 2395 (1987).

S. A. Rice: My answer to Prof. Manz is that, as I indicated in my presentation, both the Brumer–Shapiro and the Tannor–Rice control schemes have been verified experimentally. To date, control of the branching ratio in a chemical reaction, or of any other process, by use of temporally and spectrally shaped laser fields has not been experimentally demonstrated. However, since all of the control schemes are based on the fundamental principles of quantum mechanics, it would be very strange (and disturbing) if they were not to be verified. This statement is not intended either to demean the experimental difficulties that must be overcome before any verification can be achieved or to imply that verification is unnecessary. Even though the principles of the several proposed control schemes are not in question, the implementation of the analysis of any particular case involves approximations, for example, the neglect of the influence of some states of the molecule on the reaction. Moreover, for lack of sufficient information, our understanding of the robustness of the proposed control schemes to the inevitable uncertainties introduced by, for example, fluctuations in the laser field, is very limited. Certainly, experimental verification of the various control schemes in a variety of cases will be very valuable.

S. Mukamel: In relation to the report by Prof. Gerber, I would like to comment that chemical bonding can also be viewed as *electronic coherence*. By looking at the relevant single-electron density matrix in the atomic orbital representation, we note that the diagonal elements give the local charges whereas the off-diagonal elements (coherences) represent bond order. Our studies of nonlinear optical spectroscopy of conjugated polyenes have shown that, using this view, one can define electronic normal modes and view the electronic system as a collection of coupled harmonic oscillators representing collective electronic motion [1]. This is a very different picture than using the global electronic eigenstates. Using this picture, it is possible to treat electronic and nuclear degrees of freedom along similar lines. It also furnishes a very powerful means in computing optical response functions, which are size consistent [2].

1. S. Mukamel, A. Takahashi, H. X. Wang, and G. Chen, *Science* **266,** 250 (1994).

2. V. Chernyak and S. Mukamel, *J. Chem. Phys.* **104,** 444 (1996).

G. Gerber: In response to Prof. Mukamel, I should remark that the coherence between molecular electronic states induced by our intense ultrashort laser pulse is not restricted to bound states but also includes repulsive electronic surfaces. In that sense chemical bonding is related to electronic coherence.

Another somewhat different example of coherence of electronic states is a radial electronic Rydberg wavepacket whose dynamics can be studied in pump–probe experiments.

A. H. Zewail: Prof. Mukamel's point is very interesting and we should think of this different language. If I understand, the point is that bonding can be described as an "off-diagonal" density matrix. As with the nuclear motion, we now can picture the process and think of controlling the bonding.

S. Mukamel: You are absolutely correct. Although chemical bonding is a complex many-body problem, for most practical purposes, it is sufficient to look at the off-diagonal elements of the reduced single-electron density matrix. Historically, nuclear molecular motions have been treated using normal modes, whereas electronic properties are calculated using many-electron wave functions. The density matrix and its equation of motion obtained using the time-dependent Hartree–Fock theory provides a normal-mode representation of electron dynamics. The density matrix may also provide a natural extension of density functional theories, resulting in a new way for computing ground-state properties [V. Chernyak and S. Mukamel, *Phys. Rev. A* **52,** 3601 (1995)].

P. W. Brumer: As we know, in quantum mechanics, time evolution and coherence are synonymous. Thus, if I see time evolution, then coherences underlie the observation. Hence, in moving my arm I have created a molecular coherence. We should all be asking why this is so easy to create compared to the complex experiments described in these talks? Is it due to the closely lying energy levels in large systems? If so, then it suggests that experiments on larger molecules would be easier.

B. A. Hess: The reason that macroscopic motions display coherence is that they are in most cases at the classical limit of quantum dynamics. In this case, a suitable occupation of quantum states ensures that quantum mechanical expectation values equal the classical value of an observable. In particular, the classical state of an electromagnetic field (the coherent state) is one in which the expectation value of the operator of the electromagnetic field equals the classical field strengths.

M. Quack: Paul Brumer has asked why it is so easy to generate the coherent state corresponding to his waving hand compared to the difficulties of generating similar coherences in molecules by femtosecond spectroscopy. I shall give a very incomplete answer to this based on Schrödinger's interpretation [1]. For a small atomic and molecular system, the quantum energy spacings are very large, requiring large excitation bandwidths (or short times) to generate the coherences. In

a heavy-mass (macroscopic) body the quantum-level energy spacings are small, and thus it is easy to generate coherences on very long time scales.

In relation to Paul Brumer's comment that quantum mechanics surely applies also to macroscopic bodies, I would like to turn around the question, however: Why is it so difficult to generate *stationary states* or more generally *superposition states* of classically localized states? We have been interested for some time in doing this type of superposition experiment for large, chiral, polyatomic molecules [2] including "chiral" oscillator motion [3–5]. When one extends such considerations to a macroscopic classical pendulum, one must admit that we do not know whether the superposition principle of quantum mechanics applies: To date this has never been tested experimentally in such cases. Until we have experimental proof, we must leave the answer to this question open. Although there are certainly many among us who would wish to accept the validity of quantum mechanics for macroscopic bodies (classical mechanics being only a limiting law to quantum mechanics), I might point out that the validity of the superposition principle has been questioned [6] even for the superposition experiment for chiral molecules that I have mentioned above.

Again this question will have to be solved by experiment [7], although most workers in the field would certainly assume the validity of the superposition principle here. I think that there are more such open questions around than we usually wish to admit, and in *this sense* I fully agree with Paul Brumer's comment.

1. E. Schrödinger, *Naturwissenschaften* **14,** 664 (1926).
2. M. Quack, *Chem. Phys. Lett.* **132,** 147 (1986).
3. R. Marquardt and M. Quack, *J. Chem. Phys.* **90,** 6320 (1989).
4. R. Marquardt and M. Quack, *J. Phys. Chem.* **98,** 3486 (1994).
5. R. Marquardt and M. Quack, *Z. Physik D* **36,** 229 (1996).
6. P. Pfeifer, in *Energy Storage and Redistribution in Molecules* (proceedings of two workshops, Bielefeld, 1980), J. Hinze, Ed., Plenum, New York, 1983, p. 315; H. Primas, *Quantum Mechanics and Reductionism*, Springer, Berlin, 1981.
7. M. Quack, in *Energy Storage and Redistribution in Molecules* (proceedings of two workshops, Bielefeld, 1980), J. Hinze, Ed., Plenum, New York, 1983; in *Femtosecond Chemistry*, J. Manz and L. Wöste, Eds., Verlag Chemie, Weinheim, 1995, Chapter 27, p. 781.

M. S. Child: The comments of Brumer and Quack raise questions about the correspondence between classical and quantum mechanics. In this connection one must first recognize that the classical analogue of a wavepacket is not a single particle but an ensemble. Second, the

spreading of the wavepacket arises largely from the spreading of this ensemble: Quantum effects come in via interference between different components of the ensemble. Hence the oscillation of a macroscopic object such as Brumer's arm is seen as classical because the interference effects become smaller and smaller. The coherence in this case is classical in the sense that the components of the ensemble move together.

Consequently, in considering what properties of a system favor coherence, the mass or size of the species will be less important than the underlying classical coherence. We know that a harmonic oscillator is coherent classically because the oscillators of each ensemble component have the same frequency and quantum mechanically because all energy spacings are equal. Hence coherence is favored by harmonic behavior regardless of the system size.

P. W. Brumer: Several of the speakers (namely Profs. B. A. Hess, M. Quack, and M. S. Child), responding to my question, have suggested that something different happens in the classical limit. However, if we accept the idea that quantum mechanics is a generally applicable theory, then it is applicable to macroscopic systems in the classical limit. As such, dynamics and coherences are, as I said, synonymous in both the quantum and the classical limits. I favor the view of Martin Quack that the closeness of the level spacings in large systems simplifies the preparation of a superposition. Hence experiments on larger molecules seem desirable.

G. R. Fleming: When interpreting experimental signals involving coherent motion, it is necessary to distinguish ground- and excited-state behavior. The experiment is sensitive to $\delta\rho_e$ and $\delta\rho_g$. Here, $\delta\rho_e$ looks like an oscillatory wavepacket. Whether $\delta\rho_g$ looks like a pure hole, however, depends strongly on the temperature. [See D. M. Jonas et al., *J. Phys. Chem.* **99,** 2594 (1995); D. M. Jonas and G. R. Fleming, in *Ultrafast Processes in Chemistry and Biology*, Blackwell, Oxford, 1995, p. 225.]

J. Troe: Prof. Zewail, have you analyzed the "coherence" pattern observed in HgI from dissociating IHgI* with respect to the extent of "vibrational adiabaticity" of the motion downhill from the energy barrier?

A. H. Zewail: For vibrational adiabaticity we must complete the study of correlation of reaction product distribution to the nature of the initial excitation (see reply to Prof. Marcus below). You may be interested to know that for a given energy within our pulse we see tra-

jectories to the diatom at low energies (~200–300 fs) and high energies (~1–2 ps).

R. D. Levine: The coherence that is being discussed by Profs. Troe and Zewail is due to a localized vibrational motion in the AB diatomic product of a photodissociation experiment ABC → AB + C. Such experiments have been done both for the isolated ABC molecule and for the molecule in an environment. As the fragments recede, effective coupling of the AB vibrational motion to the other degrees of freedom can rapidly destroy the localized nature of the vibrational excitation.

This localization can be due to different reasons. In a femtosecond pumping experiment of the type discussed in the lecture of Prof. Zewail, the localization is due to the fast pumping. In our simulations [M. Ben-Nun and R. D. Levine, *Chem. Phys. Lett.* **203,** 450 (1993)] the initial state is located at the transition state on the top of an activation barrier and has a thermal distribution in the symmetric stretch motion. This is the motion that correlates with the vibrational coordinate in the products. As the system evolves downhill from the transition state to the products, there are many more states that can be populated because potential energy is being released. In other words, we start the system at the bottleneck in phase space, and as it evolves, the volume in phase space that is available to it grows all the time. One extreme situation is that the system is rapidly spreading over the available phase space. Another extreme is that the system evolves in a strictly vibrationally adiabatic manner, so that at every point along the reaction coordinate the vibrational distribution is a stationary one. What we observe in the simulation is yet another extreme behavior: For a significant duration (on the fast time scales of interest) the system remains quite localized in phase space but in a nonstationary state. In other words, the vibrational phase is very much nonuniformly distributed. In coordinate space this is reflected by a vibrational motion that is quite localized, just as in the femtosecond pump–probe experiment.

We have run the simulations both for a reaction in a liquid and in the isolated gas phase. On the sub-picosecond time scale the localization was essentially the same.

There are three quite distinct perturbations that could have caused the vibrational motion to delocalize. The first is that the potential that governs the vibrational motion is not harmonic and it is not harmonic either in the simulations or, of course, in the real molecule. In our experience, under most circumstances this is the effect that comes in at the earliest times. We have seen this to be the case not only for a chemical reaction but also in simulations of femtosecond pump–probe experi-

ments [M. Ben-Nun, R. D. Levine, D. M. Jonas, and G. R. Fleming, *Chem. Phys. Lett.* **245,** 629 (1995)]. The next is the vibrationally nonadiabatic coupling to the motion along the reaction coordinate. Finally there is the perturbation due to the solvent, if any. For a dipolar vibration in a polar solvent or for a vibration that is strongly coupled to the translational motion, the latter two effects will come in earlier in time. Otherwise, it is the delocalization of the vibrational distribution itself that seems to determine the time scale for vibrational coherence. It is interesting that in cases of realistic complexity the coherence can survive long enough to be observable.

A. H. Zewail: The "bottleneck" pointed out by Prof. Levine surely is related to the nature of the potential transverse to the reaction coordinate. Do you agree?

R. D. Levine: The bottleneck I mentioned is that separating reactants and products of a bimolecular reaction that has an activation barrier, that is, the saddle-point region. As the system descends from the saddle point toward the products' region, a much larger volume in phase space becomes available to it. It can sample it uniformly or it can fail to do so and remain more or less localized. One manifestation of a final nonuniform distribution that we are long familiar with is that the distribution of product quantum states is nonstatistical. Here we are talking of a complementary manifestation, namely the coherence. The effect requires an initial localization but it does not however require that this is due to the topography of the potential-energy surface. As you have demonstrated, one can create it by a ultrafast optical excitation.

R. A. Marcus: The appropriate criterion of vibrational adiabaticity in the IHgI $\rightarrow$ I + HgI reaction studied by Prof. Zewail involves the distribution of vibrational quantum states of the HgI rather than the observation of coherence in the prepared wavepacket. If an IHgI molecule were prepared in a packet of a few vibrational states, vibrational adiabaticity of the motion would imply that the HgI products would be formed in only a few vibrational quantum states. If the motion were vibrationally highly adiabatic, the final HgI packet would display large changes of vibrational quantum number. The extent of vibrational adiabaticity depends on the curvature of the reaction path and how rapidly this vibrational frequency changes along the reaction path (as discussed in some articles I wrote in 1966 [1]). Regardless of whether the reaction IHgI $\rightarrow$ I + HgI is or is not vibrationally adiabatic, a coherently vibrating wavepacket would still be observed. Only its distribution of vibrational states would differ in the two cases.

1. R. A. Marcus, *J. Chem. Phys.* **43,** 1598 (1965); **45,** 4493, 4500 (1966).

A. H. Zewail: With regard to Prof. Marcus's comment, we have observed the coherence-in-products first in the IHgI system where the wavepacket is launched near the saddle point. The persistence of coherence in products is fundamentally due to (1) the initial coherent preparation (no random trajectories) and (2) the nature of the potential transverse to the reaction coordinate (no dispersion). The issue of vibrational adiabaticity in the course of the reaction, as you pointed out, must await complete final-state analysis for well-defined initial energy. However, we do know that for a given energy of the initial wavepacket a broad distribution of vibrational coherence (in the diatom) is observed.